Review

Evaluation of the Embrittlement in RPV Steels by Means of a Hybrid NDE Approach

Gábor Vértesy *, Madalina Rabung, Antal Gasparics, Inge Uytdenhouwen, James Griffin, Daniel Algernon, Sonja Grönroos, Jari Rinta-Aho

Posted Date: 14 December 2023

doi: 10.20944/preprints202312.1008.v1

Keywords: reactor pressure vessel; neutron irradiation generated embrittlement; electromagnetic nondestructive evaluation

Review

Evaluation of the Embrittlement in RPV Steels by Means of a Hybrid NDE Approach

Gábor Vértesy[1,*], Madalina Rabung[2], Antal Gasparics[1], Inge Uytdenhouwen[3], James Griffin[4], Daniel Algernon[5], Sonja Grönroos[6], Jari Rinta-Aho[6]

[1] Centre for Energy Research, 1121 Budapest, Hungary; vertesy.gabor@ek-cer.hu; gasparics.antal@ek-cer.hu
[2] Fraunhofer Institute for Nondestructive Testing (IZFP), 66123 Saarbrücken, Germany; madalina.rabung@izfp.fraunhofer.de
[3] SCK CEN Belgian Nuclear Research Centre, 2400 Mol, Belgium; inge.uytdenhouwen@sckcen.be
[4] CU Coventry University, Coventry, UK; ac0393@coventry.ac.uk
[5] SVTI Swiss Association for Technical Inspections, 8304 Wallisellen, Switzerland; daniel.algernon@svti.ch
[6] VTT Technical Research Centre of Finland Ltd., P.O. Box 1000, FI-02044 VTT, Finland; smgronroos@gmail.com, jari.rinta-aho@helsinki.fi

Abstract: Nondestructive determination of the neutron irradiation induced embrittlement of nuclear reactor pressure vessel steel is a very important and recent problem. In the frame of the so called NOMAD project, funded by the Euratom research and training program, novel nondestructive electromagnetic testing methods were applied for inspection of irradiated reactor pressure vessel steel. In this review the most important results of this project are summarized. Different methods were used and compared with each other. Measurement results were compared with the destructively determined ductile to brittle transition temperature (DBTT) values. Three magnetic methods: 3MA (micromagnetic, multiparameter, microstructure and stress analysis), MAT (magnetic adaptive testing) and Barkhausen noise technique (MBN) were found as the most promising techniques. The results of these methods were in good confidence with each other. Good correlation was found between the magnetic parameters and the DBTT values. The basic idea of the NOMAD project is to use a multi-method/multi-parameter approach and to focus on their synergies that allows to recognise the side effects therefore supressing them at the same time. Different types of Machine Learning (ML) algorithms were tested in competition and their performances were evaluated. The important outcome of the ML technique is that not only one, but several different ML techniques could reach required precision and reliability, i.e. to keep the DBTT prediction error lower than +/-25°C threshold, which was previously not possible for any of the NDE methods as single entities. A calibration/training procedure was carried out on the merged outcome of testing methods with excellent results to predict transition temperature, yield strength and mechanical hardness for all investigated materials. Our results, achieved within NOMAD project can be useful for the future potential introduction of this (and in general, any) nondestructive evolution method.

Keywords: reactor pressure vessel; neutron irradiation generated embrittlement; electromagnetic nondestructive evaluation

1. Introduction

In majority of industrial countries, nuclear power plants (NPPs) are used worldwide to generate electricity. There are two reasons for the current use of nuclear power: increased world prices for fossil fuels and the fear of climate change due to CO2 emissions during combustion. Today 353 reactors in the world are older than 25 years among which, 154 are above 40 years. The long-term operation (LTO) of existing NPPs has already been accepted in many countries as a strategic objective to ensure adequate supply of electricity over the coming decades [1, 2]. The public and energy experts may disagree as to whether or not nuclear reactors are indispensable as an energy source for today's human society, but both supporters and opponents of nuclear energy agree that the safety of reactors must be maintained at the highest possible level.

 doi:10.20944/preprints202312.1008.v1

The design lifetimes are affected by operating conditions, such as neutron exposure (fluence), and also by magnitude and number of temperature and/or pressure cycles [3,4]. The two basic regulatory approaches are the license renewal and the periodic safety reviews, which are required for an authorization of the long-term operation of NPPs [1]. Evaluation of these parameters makes possible an estimation of the operational NPP lifetime [3].

One of the most important and irreplaceable parts that limits the lifetime of NPPs is the steel reactor pressure vessels (RPV), which encloses the extremely radioactive part of the whole system. RPV must be tough, solid, strong and absolutely reliable. It should never be cracked or leak or in any way allow the radioactive contents to escape from inside. However, it is well known, that the mechanical properties of the RPV wall are modified during the operation [5]. The ageing of the structure of the RPV steel near to reactor core is generated by long term and high-energy neutron irradiation and also, by thermal effects. These effects change the microstructure of the steel and changes the RPV material to become more and more brittle, more susceptible to unwanted cracks.

Evaluation of these parameters allows for an estimation of the operational lifetime of NPPs. Currently, destructive tests are performed on surveillance samples in the frame of periodic safety reviews (PSRs) in order to assess the material degradation induced by the neutron irradiation in RPV. Charpy impact test, which is performed on surveillance specimens is the presently applied traditional and highly reliable way of the RPV toughness inspections. Surveillance specimens are standard tensile and ISO-V Charpy specimens of exactly the same RPV steels and their welds [6]. These specimens experience exactly the same history as does the RPV steel of the vessel. It is supposed that their physical conditions are varying during the whole lifetime of the reactor in the same way as that of the vessel. Their physical condition testifies even about the "near future" condition of the vessel material.

The neutron irradiation induced embrittlement is usually described by the ductile-to brittle-transition temperature (DBTT). To obtain a single DBTT value, several specimens must be tested. For assessing structural material information over a long period, a lot of Charpy samples are needed. In parallel, tensile specimens tested under a quasistatic loading rate are used to determine yield strength, tensile strength, uniform elongation, total elongation, and reduction in diameter.

Due to possible material heterogeneities such as macro-segregated regions, hydrogen flakes, inclusion areas in such large components the surveillance specimens might not necessarily represent the whole vessel material. Furthermore, the destructive methods do not allow for the characterization of the progress of material properties of the same specimen when successively damaged. They are not applicable to the actual component and finally, the amount of surveillance Charpy samples are limited for monitoring over an elongated period.

It is evident, that a nondestructive technique of RPV steel material testing can avoid many of the aforementioned problems. It could be either a nondestructive inspection of an alternative series of surveillance specimens, which would be measured outside of the pressure vessel, then returned back into the vessel after each investigation, and measured again, at the next periodic inspection phase. Alternatively, special inspection methods and devices employing non-destructive techniques could be utilized, enabling an inside inspection of the vessel with the aid of specially equipped electrical leads. Even, a non-invasive evaluation of the vessel material could be per-formed, focusing on carefully chosen external areas of the vessel whenever feasible.

However, unlike mechanical tests, nondestructive tests do not directly measure the material property. Currently, no single nondestructive test has re-placed existing testing methods such as the destructive Charpy test.

A project ("NOMAD"), oriented towards the development of novel electromagnetic nondestructive methods for the inspection of operation-induced material degradation in nuclear power plants received funding from the Euratom research and training programme. The purpose of this review paper is to give a comprehensive survey about the results, achieved within the project. In the project a combination of several nondestructive methods was used to examine how accurately and reliably the degradation of cladded RPV material could be determined, especially when compared to sample-based destructive testing. Charpy samples, cladded and non-cladded blocks of

 doi:10.20944/preprints202312.1008.v1

various RPV steels along with different levels of irradiation states, were provided. Different non-destructive evaluation techniques were adapted and applied to measure the irradiated and non-irradiated samples. The applied NDE methods were magnetic, electrical and ultrasonic methods. Destructive reference tests for the determination of the DBTT and other material characteristics were carried out as well. The irradiated samples were handled and measured in hot cells. The measured data were evaluated and correlated with the destructively determined DBTT values using machine learning methods. In this way a predictive model was generated which is able to non-destructively determine the DBTT for various RPV steel types by intelligently combining the information of several non-destructive testing methods. The outcome of the data-driven approach was finally validated.

The validation was established by a detailed evaluation of the functionality of the NOMAD tool. This was done in the context of the regression approach as well as it was complemented by a classification approach. Furthermore, the evaluation provided insight into the relevance of the different measurement features. Based on these achievements, recommendations were made under the assumption of a continuation of the development toward a higher TRL.

A short description of the physical background of the radiation embrittlement of RPV steel is devoted in Section 2. The state-of-the art regarding nondestructive investigation before the NOMAD project is summarized in Section 3. Electromagnetic nondestructive tests of various irradiated RPV steels are summarized in Section 4. The purpose of the NOMAD project is described in Section 5. The sample preparation and description of destructive tests are described in Sections 6 and 7. The results of the measurement, performed in the project, both on Charpy and block specimens are summarized and, in addition different methods are compared with each other in Section 8. Section 9 is devoted to studying the evaluation of multi-output-parameter (i.e. combined) NDE technique with the help of advanced classification methods, particularly Machine Learning (ML) technique and its applicability. Section 10 is the discussion and interpretation of the project, while in summary and conclusions (Section 11) the summary of the whole project and recommendations are given for future research and application of the investigated techniques.

The different methods, applied in the project are described detailed in Appendix A, while in Appendix B, the interpretation of the scatter of measured points is analysed.

2. The radiation embrittlement

The main ageing process of the reactor pressure vessels is the irradiation embrittlement of the metallic structural materials. A large number of experimental and theoretical studies were published on the influence of radiation embrittlement. Several reviews were published about this phenomenon [7-18].

Radiation embrittlement is caused by the high energy fast neutron radiation (over 0.1 MeV), and high energy gamma radiation. Embrittlement refers to a decrease in the fracture toughness of reactor vessel materials and affects the vessel materials in the vicinity of the reactor fuel, referred to as the vessel's "beltline". It is one of the most significant life limiting degradation phenomena of the pressurized and boiling water reactors. Consequently, the monitoring of this ageing process is primary interest of the Nuclear Power Plant Operators and the Regulatory Bodies.

Testing and evaluation of radiation embrittlement is a difficult task. The radiation embrittlement is not one simple degradation mechanism but the sum of several processes as it is shown in Figure 1.

- direct matrix damage due to neutron bombardment (increase of the dislocation density)
- precipitation hardening of the matrix (Cu is the leading element but Ni, Mn, Si etc. also has influence)
- segregation (P is a recognized segregating element) and if P covers the grain boundary even only in one atom thickness it can cause non-hardening embrittlement.

Preprints (www.preprints.org) | NOT PEER-REVIEWED | Posted: 14 December 2023 doi:10.20944/preprints202312.1008.v1

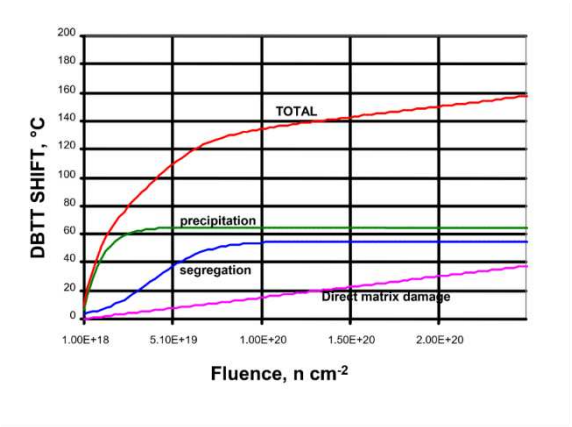

Figure 1. The processes of the radiation embrittlement. Dependence of the change in the transition temperature (DBBT) as functions of the E>0.1 MeV neutron fluence. [13].

Direct matrix damage due to neutron irradiation can be assumed to be simply root square dependent on fluence for a given material and a given temperature. At higher irradiation temperatures the rate of damage is considered to be decreasing due to increased atoms mobility. During direct matrix damage formation, Cu, together with other elements, is known to lead to precipitation mechanisms of nano-precipitates also inducing matrix hardening and embrittlement. Such mechanism continues until saturation depending on available amount of precipitants, Cu concentration in particular. In addition, other elements, like P, can segregate, in the grains (and or through diffusion processes at grain boundary) also in combination to matrix damage or attracted into the Cu-type precipitates. Diffusion of segregates also plays a role making this mechanism rather difficult to understand in detail. P segregation to the grain boundaries generally doesn't cause hardening.

The so-called Master Curve approach for assessing fracture toughness of an irradiated reactor pressure vessel (RPV) steel has been gaining acceptance throughout the world. This direct measurement approach is preferred over the correlative and indirect methods used in the past to assess irradiated RPV integrity. Experience in using results obtained from Master Curve testing has been illustrated by Wallin [19], and the approach has been applied utilizing ASTM Standard Test Method E 1921 [20] in the USA [21]. There have been comparisons made using Master Curve data in other countries, but the primary attempts at licensing implementation for nuclear reactor safety of RPVs have been in the USA.

Furthermore, several other effects have to be considered. Thermal ageing and thermal annealing are accelerated by irradiation (irradiation speeds up the diffusion processes even at relatively low temperature). These processes are time dependent; consequently, the irradiation flux rate may also affect the rate of the embrittlement. Through the cross section of an RPV wall (especially in the case of forgings) the fracture toughness properties are changing and the rate of thermal ageing is different [22-24]. Significant differences can be found in thermal expansion coefficients with respect to pressure vessel base metals, which can cause a stress peak [25]. This is the so-called pressurized thermal shock and it is a potential risk of interfacial crack initiation and propagation. Safety analysis of this phenomenon has lately become a subject of interest for operators of nuclear power plants [26].

There is a literature review available that presents the current understanding of the mechanisms behind radiation-induced embrittlement in low alloy reactor pressure vessel steels and irradiation-assisted stress corrosion cracking in the core internals of stainless steels [27].

3. NDT methods - state of art

As outlined in the previous sections, the mechanical properties of the reactor pressure vessel wall are modified during its operation. As a result, the regular inspection of nuclear power plants is an extremely important task. The DBTT, measured by destructive Charpy tests is the standardized parameter in the nuclear industry, which characterizes the embrittlement. A significant drawback of

this method is that many samples are necessarily used for this inspection. Additionally, the measurement error is high. Because of these arguments, different nondestructive methods have also been recommended and applied for monitoring the degradation of nuclear pressure vessel steel material. The life prediction and NDE of materials properties in the power plant industry was given in [28].

However, as already mentioned in the introduction, nondestructive tests cannot directly measure the material property that needs to be determined - un-like destructive methods. They can measure quantitative values of other physical properties (like different electromagnetic parameters), which are influenced by similar reasons, such as, for instance by presence and quality of structural material defects and therefore correlate with the mechanical properties. The reliable way to obtain quantitative information on a destructive-test-based required property, such as DBTT, when using nondestructive measurements, is through establishing a credible one-to-one correlation between the destructively and nondestructively measured properties. This requires series of comparative experimental investigations. All nondestructive tests must be rigorously correlated to relevant destructive tests through multiple series of checked and re-checked measurements before reliable application. This lack of correlation is the primary reason that no non-destructive test has been able to replace destructive tests, or even be applied as an auxiliary test, which could build a strong foundation for correlation verification. Nevertheless, a number of potential nondestructive tests were recommended and tested, and the mosaic of the requested correlations is presently being built up.

These tests could be done with the aid of armoured electrical leads through special bushing/containment within the vessel. Furthermore − at least in principle − it could be a nondestructive quality inspection of the vessel material itself, at different well selected positions, from outside of the vessel. Several indirect physical methods (e.g. magnetic, ultrasound, acoustic, X-rays, and others) of nondestructive testing exist, and they can be principally applied for such inspections.

Number of nondestructive methods have recently been suggested for studying the neutron irradiation-generated embrittlement of RPV steel material. Paper [29] gives a summary of electromagnetic techniques used for nondestructive testing (NDT) of degradation of nuclear reactor components. However, since neutron irradiation makes the investigated material radioactive and this causes significant difficulty in their measurement, simulation techniques, such as ion irradiation, thermal ageing and cold working, can also be used to simulate irradiation damages [30-32].

3.1 Piezoelectric Ultrasound (Piezo-US)

The well known ultrasonic method is widely applied in the inspection of NPPs [33-35]. Piezoelectric transducers use the so-called piezoelectric effect to excite ultrasonic waves. This effect is based on the occurrence of an electrical voltage when piezoelectric crystals are mechanically expanded and compressed (direct piezoelectric effect). Applying an electrical voltage to these crystals will, in turn, lead to their deformation proportional to the electric field (indirect piezoelectric effect). Thus, by using the piezoelectric effect, electrical energy is transformed into mechanical energy and vice versa. The indirect piezoelectric effect is used to transmit ultrasonic waves; the direct one is used to receive ultrasonic waves. As in this case the ultrasonic waves are generated in the transducers themselves, a coupling agent is needed to transfer these waves into the test object as well as to receive them.

The ultrasonic time-of-flight (TOF) method can be used as well, as the main measured quantity of the ultrasonic testing method. The TOF is defined as the time the ultrasonic wave requires for propagating from transmitter to receiver. For a given wave mode, microstructure changes and mechanical properties influence the effective ultrasound velocity and, therefore, they affect the TOF. The TOF is determined by fitting a peak of the received waveform with a parabolic function and determining the peak position analytically. The achievable accuracy lies in the single-digit nanosecond range [36, 37].

3.2. Electrical methods

 doi:10.20944/preprints202312.1008.v1

3.2.1. Thermoelectric power measuring method (TEPMM)

Thermoelectricity is based on the fact that a thermal flux driven by a temperature gradient in an electrically conductive material is accompanied by an electric current. The voltage or thermoelectric power (TEP) created hereby is proportional to the temperature gradient. The material-dependent proportionality factor is called Seebeck coefficient (SC). Today, thermoelectric devices as temperature sensors (thermocouples), heat sources or sinks and remote power generators are based on thermoelectric effects and widely used. The change of the SC due to neutron irradiation, thermal and mechanical ageing was observed experimentally. These effects are well known as a cause of drift in thermocouples, which are widely used as temperature sensors [38-40].

3.2.2. Direct current-reversal potential drop (DCRPD)

Four-point probe direct current-reversal potential drop (DCRPD) method is based on the measurement of electrical resistivity of metal. Material property changes in irradiated RPV can be used as indicators for the state of the degradation. One physical effect that can be used for the detection of irradiated material degradation is the electrical resistivity. If the change of electrical resistivity is a well-defined function of the neutron fluence, and if the effect is large enough compared with that of other influencing parameters, it can be used the monitor the material embrittlement. The development and testing is done to investigate the suitability of electrical resistivity measurement for the characterization of the irradiation embrittlement in irradiated pressure vessel steel. Characterizing irradiated RPV base metal, electrical resistivity requires measurement of very low resistance changes with high accuracy [41,42].

3.3. Magnetic methods

The majority of the nuclear reactors, which are used presently are pressurized water reactors. The steel used in the reactor pressure vessel is ferromagnetic, allowing for effective inspection using magnetic methods. Magnetic nondestructive methods are an important part of all the possible techniques, especially because of their simplicity. Furthermore, it is known and understood that magnetic and mechanical properties of ferromagnetic materials are very closely correlated: regularity of microstructure of ferromagnetic construction materials (e.g. of RPVs) and density and quality of its defects, has a significant influence on both the mechanical and magnetic properties of the material. Domain wall motion and dislocation movement are both influenced by the microstructure of the material. The correlation between mechanical and magnetic hardness in ferromagnetic materials is well-known and understood [43,44]. The practical applicability of magnetic methods for quantitative indication of steels micro-structural modifications resulting embrittlement were proved by numerous successful measurements.

In [45-49] overviews can be found about nondestructive magnetic methods. These papers provide guideline to the literature of magnetic techniques for nondestructive material testing. Compared to other NDE techniques such as ultrasonics or eddy currents, the literature on magnetic methods is limited, yet one of the challenges is its wide-spread dispersion. The above mentioned reviews present a fairly comprehensive summary of works on the known methods, such as Barkhausen noise effect, magnetoacoustic emission, magnetic hysteresis method, residual field and magnetically induced velocity change methods that can be used in practice.

The well-known magnetic Barkhausen noise technique (MBN) was originally developed for inspection of surface defects, of residual stresses and of microstructure changes [50]. There is a wide choice in the literature how MBN can be applied for material characterization [51-60].

Magnetoacoustic emission, another magnetic method, can also be successfully used for the monitoring of residual stresses [61,62].

A nondestructive magnetic method was previously developed, which is called as 3MA approach (3MA = micromagnetic, multiparameter, microstructure and stress analysis) and this technique uses different methods [63-65].

 doi:10.20944/preprints202312.1008.v1

The measurement of the magnetic hysteresis loops is also among the perspective candidates of magnetic NDE. Theory of ferromagnetic hysteresis is given in several papers, see [66] as an example.

The magnetic hysteretic characterization of ferromagnetic materials with objectives towards NDE of material degradation was discussed in [67].

In [31] cold rolling was applied to generate crystalline defects in RPV steel. Magnetic hysteresis measurement together with Vickers hardness and tensile properties measurements were performed. The variations of remanence, hysteresis loss and coercivity were discussed in detail. It was found that the strength, the hardness and the coercivity increased with increasing deformation. A good linear correlation between the increment of coercivity, hardness and yield strength was found.

In traditional measurements of magnetic hysteresis, the major loop is measured, and several characteristic parameters, like remanence magnetization, coercive force, maximal permeability are determined from the major loop. However, in recently developed novel methods, the series of minor loops are measured instead the major loop, and a lot of different parameters of minor hysteresis loops are used for material characterization. One of these novel methods is the magnetic minor loops power scaling laws (PSL) [31, 68]. A similar method, called magnetic adaptive testing (MAT) also measures systematically the minor magnetic hysteresis loops [69-71]. As it was demonstrated, all 3MA, PSL and MAT methods are multi-parametric, powerful and sensitive method of magnetic inspection. In case of MAT method systematic comparisons were made between different magnetic nondestructive techniques: different methods – full hysteresis loop measurement, MAT and MBN – were applied in series of plastically deformed transformation induced plasticity (TRIP) steel specimens, and the results of these methods were compared with each other [72]. As a conclusion:

Good correlation was found between magnetic parameters, measured by different techniques, which is a direct proof that all magnetic methods accurately characterize the material degradation.

MAT seems to be the most sensitive method among the other investigated ones.

Good correlation was also found between magnetic parameters and with the destructively measured Vickers hardness values. This fact makes possible the future potential use of magnetic methods in the inspection of RPVs' structural integrity.

All of these parameters were determined without magnetic saturation of the investigated samples. This fact is very important in practical applications.

In the next section it will be reviewed, how these methods have been applied for investigation of the material degradation, caused by neutron irradiation.

The methods 3MA, MAT and MBN were applied in the NOMAD project.

4. Magnetic nondestructive tests of various neutron irradiated RPV steels - State of art

The practical applicability of magnetic methods have been proved recently by several successful measurements. These methods are suitable for quantitative indication of micro-structural modifications of RPV steel, causing steel embrittlement. Based on these results the future potential application of magnetic methods seems to be promising in the inspection of RPVs' structural integrity. Possibilities and difficulties of the NDE evaluation of irradiation degradation is analysed in Ref. [73]. There is a comprehensive summary about the investigation of the hardening in neutron irradiated and thermally aged iron-copper alloys, on the basis of mechanical and magnetic relaxation phenomena in Ref. [74]. In this subsection the results, which were achieved in the area of magnetic nondestructive tests of various irradiated RPVs are shown, with separated results for each of the applied methods.

4.1. Major hysteresis loop measurements

The modification of the magnetic hysteretic behaviour generated by neutron irradiation was studied for different materials in [75]. Two parameters of the hysteresis loop (maximum relative differential permeability and peak intensity of interaction field) were determined as a function of neutron fluence. A decreasing trend (change up to 40%) was found in magnetic parameters during embrittlement, regardless the origin of the embrittlement.

 doi:10.20944/preprints202312.1008.v1

The influence of the neutron irradiation on the M-H magnetization curve of the RPV material was studied in [76]. The saturation and the residual magnetic induction and the initial magnetic susceptibility were determined. It was found that the clockwise variation of the magnetization of the hysteresis curves before irradiation was lower than than after irradiation. Furthermore, the magnetization of the specimens before and after irradiation were not sensitive to temperature changes. The residual magnetization intensity was found as linearly related to the irradiation fluences less than 0.154 dpa. An exponential relationship of initial magnetic susceptibility with the radiation fluence was found as well.

The modification of saturation magnetization of RPV steel, caused by neutron irradiation was studied in [77]. Magnetic and metallurgical properties were investigated by hysteresis loop and ferromagnetic resonance (FMR) techniques. Saturation magnetization of neutron-irradiated steel increased. To explain the cause of this increase, FMR experiments were also conducted and a large difference was experienced in the resonance fields of non-irradiated and irradiated samples.

Irradiation-generated changes in the magnetic behaviour and in the mechanical properties were measured and compared in RPV forging and weld surveillance Charpy specimens to reveal the possible correlations between them [78]. The samples were irradiated by E>1.0 MeV energy neutrons up to the fluence of 2.3×10^{19}n cm^{-2}. Tensile and Charpy impact tests and Vickers microhardness measurements were carried out as mechanical parameters. Magnetic parameters, such as saturation magnetization, remanence, coercivity and Barkhausen noise amplitude were determined for none irradiated and for irradiated specimens. Hysteresis loops were found to turn clockwise, which resulted an increase in coercivity. Barkhausen noise amplitude decreased after irradiation. These magnetic parameters revealed correlation with the changes of mechanical parameters.

Recently, research on magnetic methods to investigate the neutron irradiation embrittlement processes of RPV steel have been focused mainly on Barkhausen emission measurements, and on minor hysteresis loop measurements as will be discussed in next subsections.

4.2. Barkhausen emission measurements

Promising results were achieved in the field of magnetic nondestructive tests of irradiated RPV steel also by applying Barkhausen emission measurements. One of them was already mentioned in previous sub-section [59].

As shown in [79], the measurement of Barkhausen emission can reveal neutron irradiation caused degradation in pressure vessel this parameter were in the range of −20% to −45% in case of fluences up to 25×10^{18} n/ cm^{-2} .

MBN and magnetomechanical acoustic emission were applied in Mn–Mo–Ni pressure-vessel steels, having different microstructures for studying the influence of microstructural changes on these parameters [80]. The measured signals were significantly affected the microstructural features. MBN energy varied inversely with hardness and it depended also by the microstructure. The results indicated that these quantities were closely related to the dislocation density and residual stress which.

Barkhausen noise measurements were used for the investigation of the radiation damage and thermal recovery of irradiated RPV steel samples [81]. There were identified two recovery stages from the hardness measurements results. This effect resulted from isochronal annealing, and it was presumed to be accountable for it. The mechanism can be explained by using the results of MBN measurement on the basis of the interaction between radiation induced defects and the magnetic domain wall. Irradiation caused an increase in the maximum magnetic induction, but the coercivity was not modified by neutron irradiation. MBN parameters associated with the magnetic domain wall motion decreased due to neutron irradiation, and they recovered with subsequent heat treatments.

Papers [82,83] deal with the use of MBN measurements to study the irradiation effects on nuclear reactor structural materials. Different RPV materials were investigated, and the specimens were irradiated with different neutron fluences. A stabilised flux mode was used, the magnetic flux within the sample was controlled to compensate for leakage and variations on the flux. Anisotropy effect caused by the sample cutting direction was found, which masked the magnetic signal induced by the

 doi:10.20944/preprints202312.1008.v1

irradiation effects. Specimens cut in the same direction correlate with irradiation-generated material hardening and its dependency on fluence. It was found that different materials resulted in different hardening levels. MBN parameters were correlated to neutron fluence by taking into account the cutting direction.

Microstructure effects on MBN emission and on first-order reversal curve (FORC) analysis was studied in ferritic/martensitic alloy (HT-9), which can be interesting for the experts in nuclear materials [84]. It was found that MBN emission and reversible component of magnetization, determined from the FORC data, decreased with increasing mechanical hardness. The results were discussed in terms of the use of magnetic signatures for use in NDE of radiation damage and other microstructural changes in ferritic/martensitic alloys. It is shown in this work, that FORC analysis is particularly useful for characterization of defect density and pinning, which can be correlated to bulk NDE field measurements such as MBN emission.

4.3. *Measurement* of minor hysteresis loops

By applying the magnetic minor loops power scaling laws (PSL), neutron irradiation generated modification of minor loops was found in pure Fe and in different model alloys [85]. Minor hysteresis loop coefficients which were determined from scaling relations between minor-loop parameters and in proportion to internal stress decreased in all materials, irradiated by a neutron fluence of 3.32×10^{19} n cm^{-2}. The decrease of the coefficients was found to be larger for alloys containing Cu, and it is enhanced by 1% Mn addition. This decrease can be caused by the reduction of internal stress during irradiation. It is in contrast with the changes of yield strength after neutron irradiation, which is increasing with Cu and Mn contents. In this paper, a qualitative explanation can be found on the basis of the preferential formation of Cu precipitates along pre-existing dislocations, which decreases internal stress of the dislocations.

The same PSL method was used for the measurement of low carbon steel and Fe metal, which were irradiated at 563K in a 50MW nuclear reactor [86]. Special attention was devoted to minor-loop coefficients investigating the nucleation mechanism of copper precipitates and dislocation loops during neutron radiation. The minor-loop parameters was found to be very sensitive to lattice defects, such as dislocations, copper precipitates, and grain boundaries. The minor-loop coefficients increased monotonously with the increase of neutron fluence in Fe metal. Here the dislocation loops has an important role for the brittleness.

Minor magnetic hysteresis loops were also measured on A533B-type RPV steels having various combinations of Cu and Ni content. Samples were irradiated by neutrons to a fluence up to $3.32\text{x }10^{19}$ n cm^{-2} [87]. There was found a strong compositional dependence in the minor-loop coefficient, which is obtained from a scaling power law between minor-loop parameters. This is due to the internal stress. A large increase was found in the low fluence regime (below $0.4\text{x}10^{19}$ n cm^{-2}) in the properties of high Ni and high-Cu steel, which was followed by a slow decrease. However, in low Ni and low-Cu content steel, a sudden decrease was experienced. These variations are mostly in a linear relationship with changes in yield strength. The results were interpreted from the viewpoint of the formation and growth of Cu-rich precipitates and/or fine scale defects in the matrix and along pre-existing dislocations. A model analysis, assuming Avrami-type growth of Cu-rich precipitates and an empirical logarithmic law for relaxation of residual stress demonstrated that an increment of the coefficient due to Cu-rich precipitates increased with Cu and Ni contents and was in proportion to a yield stress change, related to irradiation hardening [88,89].

In [90] the applicability of MAT, an alternative way of minor hysteresis loop measurement is demonstrated for the inspection of neutron irradiation embrittlement in RPV steels. Three series of samples (JRQ, 15CH2MFA and 10ChMFT type steels), irradiated by E > 1 MeV energy neutrons with total neutron fluence of 1.58 – $11.9 \text{ x } 10^{19}$ n cm^{-2} were investigated by this method. Correlation was demonstrated between the MAT parameters and the neutron fluence in all types of the investigated materials. Shift of DBTT as a function of the neutron fluence for the 15CH2MFA type material was also evaluated. In this case, a sensitive, linear correlation was found between DBTT and MAT parameters. Based on these results, MAT was shown as a promising, complimentary tool of the

 doi:10.20944/preprints202312.1008.v1

destructive tests within the surveillance programs, currently used for the inspection of neutron-irradiation-generated embrittlement of RPV steels. It was also found that the sensitivity depended also on the structural anisotropy due to the original direction of the material rolling/forging. The samples magnetized along the original direction of steel rolling provided the most sensitive results. Another conclusion of these measurements was that the magnetic properties of the samples were affected by the quality of the magnetic contact between the sample surface and the attached soft magnetic yoke. It was concluded that if the yoke was not in good contact with the sample surface, the results would be strongly influenced.

In other work [91] three methods (MBN emission measurements, PSL and MAT) were compared with each other on the same series of neutron irradiated RPV steel material. JRQ and 15Kh2MFA material and 10KhMFT type welding steels (for WWER 440-type Russian reactors) were used for the measurements, which were irradiated by high-energy (>1MeV) neutrons with up to 11.9×10^{19}n cm^{-2} fluences. MAT was found as the most sensitive method among the investigated techniques. It revealed the most straightforward linear correlation with the independently measured DBTT values. The other magnetic methods (MBE and PSL) were found to be less sensitive than MAT, and also, they did not correlate with DBTT, nor with each other. Considering that both MBN and PSL are highly structure-sensitive magnetic methods, the lower sensitivity and their poor correlation with DBTT can be primarily attributed to the different sensitivity to lattice defects from that of DBTT. It was also concluded, similarly to experiences in [90], that an uncontrolled fluctuation of surface quality of the slightly corroded specimens made the measurement difficult. Contact-less ways of investigating of more conveniently shaped irradiated nuclear pressure vessel steel samples was suggested for future inspections.

The influence of the rough surface on MAT measurements was carefully analysed in [92], and it was found that this harmful effect could be significantly reduced by applying a non-magnetic spacer between the sample surface and the magnetizing yoke.

4.4. Electromagnetic NDT techniques

3MA method (micromagnetic, multiparameter, microstructure and stress analysis) has been found as a suitable tool for the characterization of the degradation of ferromagnetic materials (like RPV steels).

The microstructure of the steels is modified by the neutron induced embrittlement. This phenomenon depends on the neutron fluence but also on the special design of the RPV of nuclear power plants. Embrittlement contributes to the increase of hardness and strength on the basis of vacancies and Cu-rich precipitates, and also to the shift of the DBTT to higher temperatures. Micromagnetic investigations were done at full Charpy specimen and material of the last generation of German NPP in order to characterize the material degradation [93]. This contribution reports on the results obtained by the application of the 3MA method and the magnetostrictive excitation of ultrasound using an EMAT. Both technologies document potential to be further developed to an in-service inspection technique.

By using the electromagnetic non-destructive techniques the ability of characterization of material ageing was demonstrated [94]. Thermal degradation causes hardness enhancement and appearance of Cu precipitation. An early warning can be done before fatigue life is elapsed due to Low Cycle Fatigue.

By using the micromagnetic non-destructive techniques the ability of characterization of material ageing was demonstrated [94]. Thermal degradation causes hardness enhancement and appearance of Cu precipitation. An early warning can be done before fatigue life is elapsed due to Low Cycle Fatigue.

The DBTT shift was indicating when material degradation was at well-defined laboratory-type specimens. A high sensitivity and confidence in the results was obtained. As the special application of EMAT sensors demonstrated its reliable use at a service temperature of 300 ^{o}C, the integration of this sensor type into plant lifetime management systems is an engineering problem. The purpose is

 doi:10.20944/preprints202312.1008.v1

to solve the proper selection of cooling devices for the driving microelectronic systems and to apply heat resistant wires for coils and cables especially isolated for high temperature access.

5. NOMAD Project

As it is outlined in the introduction, the long-term operation (LTO) of existing nuclear power plants (NPPs) has already been accepted in many countries as a strategic objective to ensure adequate supply of electricity over the coming decades. In order to estimate the remaining useful lifetime of NPP components, LTO requires reliable and accurate tools. To achieve a step forward in this important area, a joint research work was initiated by ten different laboratories from seven different European countries. The project (Non-destructive Evaluation System for the Inspection of Operation-Induced Material Degradation in Nuclear Power Plants, or, NOMAD for short) has received funding from the Euratom research and training programme 2014-2018 under grant agreement No 755330. The common work started in 2017 [95].

The objective of NOMAD was the development, demonstration and validation of a NDE tool for the local and volumetric characterisation of the embrittlement in operational reactor pressure vessels (RPVs). In order to address these objectives, the following steps were taken:

- Development and demonstration of an NDE tool for the characterisation of RPV embrittlement, especially accounting for material heterogeneities and exceeding the existing information from surveillance programmes.
- Extension of the existing database of RPV material degradation by adding correlations of mechanical, microstructural and NDE parameters as well as including quantification of reliability and uncertainty.
- Application of the developed tool to cladded material resembling the actual RPV inspection scenario.

The project NOMAD took into account the priorities of reactor operation, responding to stringent safety requirements from regulators, and sought to foster the convergence of nuclear safety approaches. The approach developed within NOMAD delivers information complementary to and exceeding the information obtained by destructive tests of surveillance samples, which are currently assumed to represent the whole component and do not take into account possible local material variations. NOMAD's aim was to fulfil requirements for nuclear safety in the framework of assessment for lifetime operation.

In the previous section different application possibilities of several novel – mainly magnetic – nondestructive methods are reviewed. As it is seen, good results were achieved, how these methods could be applied for the inspection of neutron irradiation generated embrittlement of RPV steel. However, only few of them were done on mechanically intact RPV steel, which would form a continuous series from not-irradiated samples up to samples of the same RPV material having the same shape, which would be subjected to high fluence of neutrons in a nuclear reactor. Hence, it can be stated that presently there is no really effective nondestructive method for radiation embrittlement evaluation in practical use. One of the reasons of the contradictory results is that the investigated irradiated specimens were mostly collected from different surveillance programs. Furthermore the investigated specimens were often mechanically deformed, sometimes corroded, and in several cases the zero level specimens were missing, or they were cut from different parts of the material.

Within NOMAD project several different nondestructive techiques were applied to detect the neutron irradiation generated material degradation in many different RPV steel materials, having either Charpy geometry or larger, cladded or non-cladded blocks. The same series of samples were measured before and after neutron irradiation, and the results, obtained by different methods were compared with each other. The purpose was to reveal the benefits and drawbacks of different methods, and finally to find, which techniques are suitable for future, practical applications. The parameters extracted from different methods were compared with the destructively measured DBTT values. A combination of several NDE methods has been used to examine how accurately and reliably

 doi:10.20944/preprints202312.1008.v1

the degradation of RPV material can be determined, especially when compared to sample-based destructive testing.

Charpy samples, cladded and non-cladded blocks of various RPV steels and irradiation states were provided. NDE techniques were adapted and applied to measure the irradiated and non-irradiated samples. The applied NDE methods were the magnetic methods MAT, 3MA-X8, MBN, the electrical methods DCRPD, TEP and the ultrasonic method Piezo-US. They were used to characterise the microstructure changes and the variation of the material properties as a function of progressing exposure (fluence level). Table 1 gives an overview on the NDE methods applied to different specimen geometries (Charpy and blocks) within the project.

Destructive reference tests for the determination of the DBTT and other material characteristics were carried out. The irradiated samples were measured and the data were correlated with the DBTT values by using machine learning methods.

The ultimate goal was to produce a machine learning-based computational tool that can estimate the neutron irradiation-induced embrittlement of reactor pressure vessel steel alloys based on the NDE parameters. This would revolutionize the current surveillance procedures, which rely heavily on destructive methods.

The non-destructive characterization was carried out by means of micromagnetic, electrical and ultrasonic methods at various stages of material degradation caused by neutron irradiation. They were used to characterise the microstructure changes and the variation of the material properties as a function of progressing exposure (fluence level). Table 1 gives an overview on the NDE methods applied to different specimen geometries (Charpy and blocks) within the project.

Table 1. NDE methods applied for the embrittlement characterization

NDE method	Charpy samples	Blocks
Micromagnetic multiparameter microstructure and stress analysis (3MA-X8)	√	√
Piezoelectric Ultrasound (Piezo-US)	√	not applicable
Direct Current-Reversal Potential Drop (DCRPD)	√	not applicable
Micromagnetic Inductive Response & Barkhausen Emission (MIRBE)	√	√
Magnetic adaptive testing (MAT)	√	√
Thermoelectric power (TEP)	√	√

In the following chapters the results of NOMAD project will be presented and analyzed.

6. Materials

Several sets of samples with various irradiation and embrittlement conditions were provided. The first specimen set consists of ISO-V Charpy samples of the four materials 18MND5 (weld), 22NiMoCr37, HSST-03 (A533-B) and A508-B. These were existing samples from previous CHIVAS - surveillance programs, which were available in non-irradiated states and in two or three irradiation states. The second specimens set consists also of ISO-V Charpy samples of the two materials A508Cl.2 and 15kH2NMFA. The A508Cl.2 was cut out from ¾ depth of a large part of the Lemoniz reactor vessel, a Spanish reactor of Western type that was never operated, [96,97]. The 15kH2NMFA material was cut out from original eastern 1000 MW RPV from the ¼ depth. The 15Kh2NMFA (CrNiMoV) forging steel was manufactured by the Russian IZHORA company for a 1000 MW WWER reactor. The original heat number is 181358 and the forging steel was produced according to the Russian specification TU 108.765-78. These Charpy samples were irradiated at three well-defined levels at the

Preprints (www.preprints.org) | NOT PEER-REVIEWED | Posted: 14 December 2023 doi:10.20944/preprints202312.1008.v1

Belgium Reactor BR2. The neutron irradiation was performed in a specially designed rig where 24 Charpy specimens were directly irradiated [98]. The second set of specimens could be non-destructively measured before and after irradiation, so an evaluation of the progressive change of the embrittlement could be performed. Table 2 shows the corresponding material compositions.

Table 2. Material compositions (wt %)

Material	C	Mn	P	Cr	Mo	Ni	Cu	S	Si
18MND5-W	0.09	1.21	0.018	0.12	0.49	0.96	0.13	0.007-0.011	0.23-0.31
22NiMoCr37	0.2	0.87	0.009	0.39	0.49	0.85	0.06	0.007-0.011	0.23-0.31
A508-B	0.2	1.4	0.01	0.1	0.45	0.74	0.06	0.007-0.011	0.23-0.31
HSST-03	0.25	1.42	0.013	0.48	0.62	0.12	0.12	0.007-0.011	0.23-0.31
A508 Cl.2	0.21	0.75	0.01	0.39	0.6	0.8	0.12	0.007-0.011	0.23-0.31
15kH2NMFA	0.16	0.42	0.012	1.97	0.52	1.29	0.12	0.007-0.011	0.23-0.31

Finally, in order to characterize the neutron-irradiation induced embrittlement through the cladding, a third specimen set was chosen consisting of six cladded and six non-cladded blocks of Western RPV material A508 Cl.2 (See also in Table 2). They are more representative for in-situ vessel inspection than the standard test Charpy samples, and has been fabricated and irradiated over a large range of neutron fluences at BR2. One part of the block samples without cladding was made of compact material cut out of the mid area of a real RPV, whereby another part of the block samples with cladding was cut out from the cladded surface of the RPV. So, the latest can be used to examine the capability of the non-destructive measuring methods for testing the irradiation induced material degradation through the cladding. The dimensions of both types of block samples are shown in Figure 2.

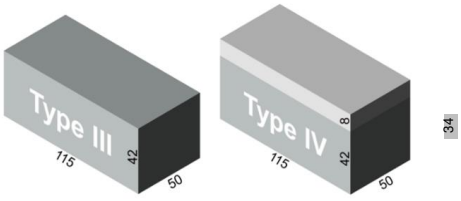

Figure 2. Dimensions (in mm) of the noncladded and cladded block samples.

These blocks were irradiated at three defined levels within BR2 similarly to the second specimens set. Two different strategies have been applied for the irradiation. The first one aimed to achieve an as uniform as possible neutron fluence profile and was applied on three cladded blocks and three, non-cladded blocks. The second one aimed to achieve damage that is much more realistic since the blocks have experienced a fluence attenuation profile.

7. Mechanical testing

Charpy impact tests were performed on all of the samples previously investigated non-destructively in order to determinate the DBTT. For the determination of DBTT of the blocks, Charpy samples have been cut out from the top layer as well as from the bottom layer. By this procedure individual DBTT values for both sides of the block specimens could be provided. The results of the mechanical testing for all three specimens sets are shown in the Tables 3, 4 and 5.

For the CHIVAS-samples (first sample set) it is visible that the DBTT is not strongly correlated with the real fluence level. Probably the overlapping varying fluence temperature may cause an annealing effect, which reduces the influence of the irradiation.

Preprints (www.preprints.org) | NOT PEER-REVIEWED | Posted: 14 December 2023 doi:10.20944/preprints202312.1008.v1

For the Charpy and block samples (second and third sample set) where the irradiation temperature was constant it can be seen that there is a strong correlation between the fluence level and the DBTT for the samples with 0, low and medium fluence. However, for the samples with medium and high fluence there is no more increasing of the DBTT. There is a clear saturation effect.

Table 3. Results of the Charpy impact tests.

Material	Fast neutron fluence [n/cm²]*E-19	Irrad. temp. [°C]	DBTT [°C]	Number of samples
18MND5-W	0	-	-51	5
	2.88 – 3.87	150	145	6
	4.57 – 5.05	260	98	3
	8.57 – 9.89	260	178	6
22NiMoCr37	0	-	-62	3
	2.99 – 4.02	260	-6	6
	4.87 – 6.84	260	29	6
HSST-03	0	-	-6	5
	2.43 – 2.80	150	161	7
	3.55 – 4.40	305	34	7
A508-B	0	-	-55	5
	3.80 – 4.39	150	156	7
	3.28 – 4.99	305	-5	8
A508 Cl.2	0	-	-33	12
	1.55	100	76	4
	4.38	100	125	4
	7.04	100	126	4
15kH2NMFA	0	-	-51	12
	2.78	100	88	4
	6.83	100	136	4
	7.9	100	124	4

Table 4. Results of the Charpy impact tests on specimens cut out from the blocks: cladded blocks top side and bottom side.

	Real Fluence [n/cm²]* E-19	Irrad. temp [°C]	DBTT [°C]	Number of samples
A508 Cl.2 Cladded topside uniform	0	-	-45	3
	2.09	100	90	1
	6.93	100	112	1
	12.70	100	112	1
A508 Cl.2 Cladded topside attenuated	0	-	-45	3
	1.48	100	94	1
	5.12	100	103	1
	8.86	100	110	1
A508 Cl.2 Bottom side uniform	0	-	-45	3
	1.72	100	119	1
	6.76	100	145	1

Preprints (www.preprints.org) | NOT PEER-REVIEWED | Posted: 14 December 2023 doi:10.20944/preprints202312.1008.v1

	12.75	100	165	1
A508 Cl.2 Bottom side attenuated	0	-	-45	3
	4.55	100	133	1
	11.23	100	157	1
	17.40	100	181	1

Table 5. Results of the Charpy impact tests on specimens cut out from the blocks: noncladded blocks.

	Real Fluence [n/cm²]* E-19	Irrad. temp [°C]	DBTT [°C]	Number of samples
A508 Cl.2 Cladded topside uniform	0	-	-45	3
	2.09	100	90	1
	6.93	100	112	1
	12.70	100	112	1
A508 Cl.2 Cladded topside attenuated	0	-	-45	3
	1.48	100	94	1
	5.12	100	103	1
	8.86	100	110	1
A508 Cl.2 Bottom side uniform	0	-	-45	3
	1.72	100	119	1
	6.76	100	145	1
	12.75	100	165	1
A508 Cl.2 Bottom side attenuated	0	-	-45	3
	4.55	100	133	1
	11.23	100	157	1
	17.40	100	181	1

8. Experimental results

8.1. Measuring procedure

In order to guarantee reproducible measurements and a stable sample-probe coupling, sample/probe holders were constructed for each NDE technique. These were relevant especially for measuring the irradiated samples in the hot cell by the mechanical manipulation for handling and positioning the samples onto the NDE probe.

In order to define a unique way to perform all NDE measurements, an inspection and quality assurance procedure was defined. According to this procedure, each sample was measured five times, each time picking up the probe and replacing it on the sample. Although sample/probe holders were used the remaining scattering caused by the handling could be averaged by the repetitions.

As the measuring activities were spread over three years it was necessary to monitor the stability and functionality of the measuring NDE devices and probes. Therefore calibration samples were defined and were periodically measured by NDE. The analysis of the resulting outcome of these NDE measurements yields to the conclusion that all NDE results are stable over the time.

 doi:10.20944/preprints202312.1008.v1

8.2. Description of the NDE of embrittlement

8.2.1. Charpy specimens

Generally, it has been observed that the outcome of the individual NDE measurements performed on different Charpy samples of the same material and the same irradiation condition scatter. Figs. 3- 8 give an overview about the measuring results for each set of Charpy specimens and for each NDE method in dependency on the corresponding DBTT. A possible explanation of this scattering lies in different origin of the samples having the same irradiation condition and, consequently, slightly different material properties before irradiation. (This effect is discussed in detail in Appendix B). This causes different progress of the material properties during neutron irradiation. Long-term repetition measurements carried out during the measurement campaigns on a reference sample showed stable results. Uncertainty studies were performed in order to find out the origin of this scatter. These studies concluded that the uncertainty of the samples can be estimated to be higher than the uncertainty of the "inspection system" [99]. Nevertheless, correlation of the nondestructively extracted features with embrittlement have been identified. Several trends correlate with each other and deliver complementary information regarding the material properties. It was expected that the NDE features show either a continuously increasing or a continuously decreasing trend for a certain material. This behaviour cannot be confirmed in case of all materials (see Figure 6 - material HSST03).

Moreover, it was observed that the same NDE feature shows different trends for different materials: Seebeck coefficient is expected to increase with embrittlement. However it decreases in case of the materials A508b and HSST03 irradiated at 305°C compared with the non-irradiated condition.

The behaviour of the NDE features is affected by both the irradiation fluence and the irradiation temperature. The increase of the fluence causes an increase of the embrittlement. The increase of the temperature has different effects on some of the NDE features: whereas temperatures below 260°C have the same influence like the irradiation fluence, it seems that higher temperatures have a contrary effect especially on the ultrasonic (US) method and Seebeck coefficient measurement (TEPMM).

In the case of the 3MA method only the most significant feature of the 21 measured features are shown. (In these figures the terminology "Micromagnetic Inductive Response & Barkhausen Emission (MIRBE)" is used for the Barkhausen noise measurements".)

Preprints (www.preprints.org) | NOT PEER-REVIEWED | Posted: 14 December 2023 doi:10.20944/preprints202312.1008.v1

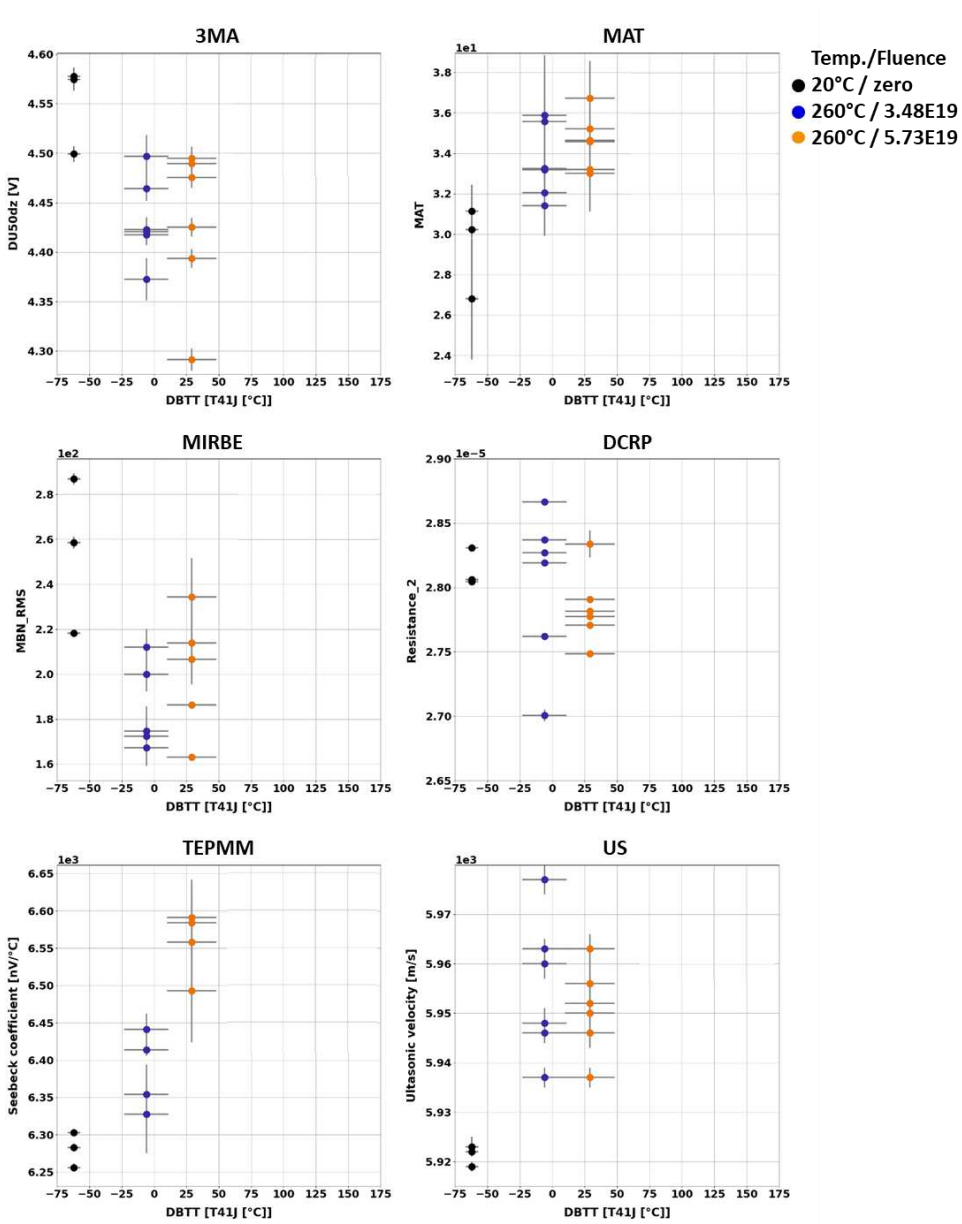

Figure 3. NDE features measured on Charpy samples of 22NiMoCr37.

Preprints (www.preprints.org) | NOT PEER-REVIEWED | Posted: 14 December 2023 doi:10.20944/preprints202312.1008.v1

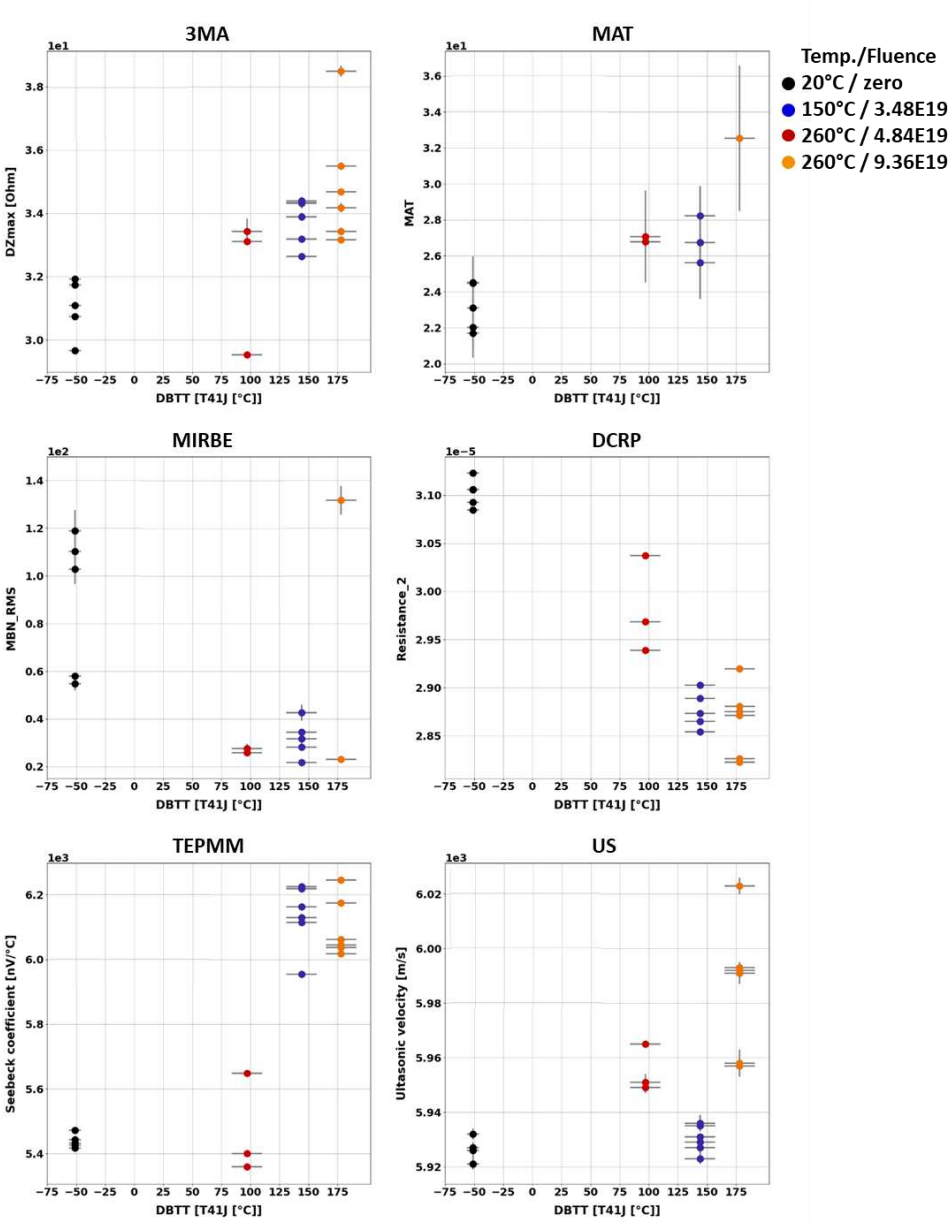

Figure 4. NDE features measured on Charpy samples of 18MND5-W.

Preprints (www.preprints.org) | NOT PEER-REVIEWED | Posted: 14 December 2023 doi:10.20944/preprints202312.1008.v1

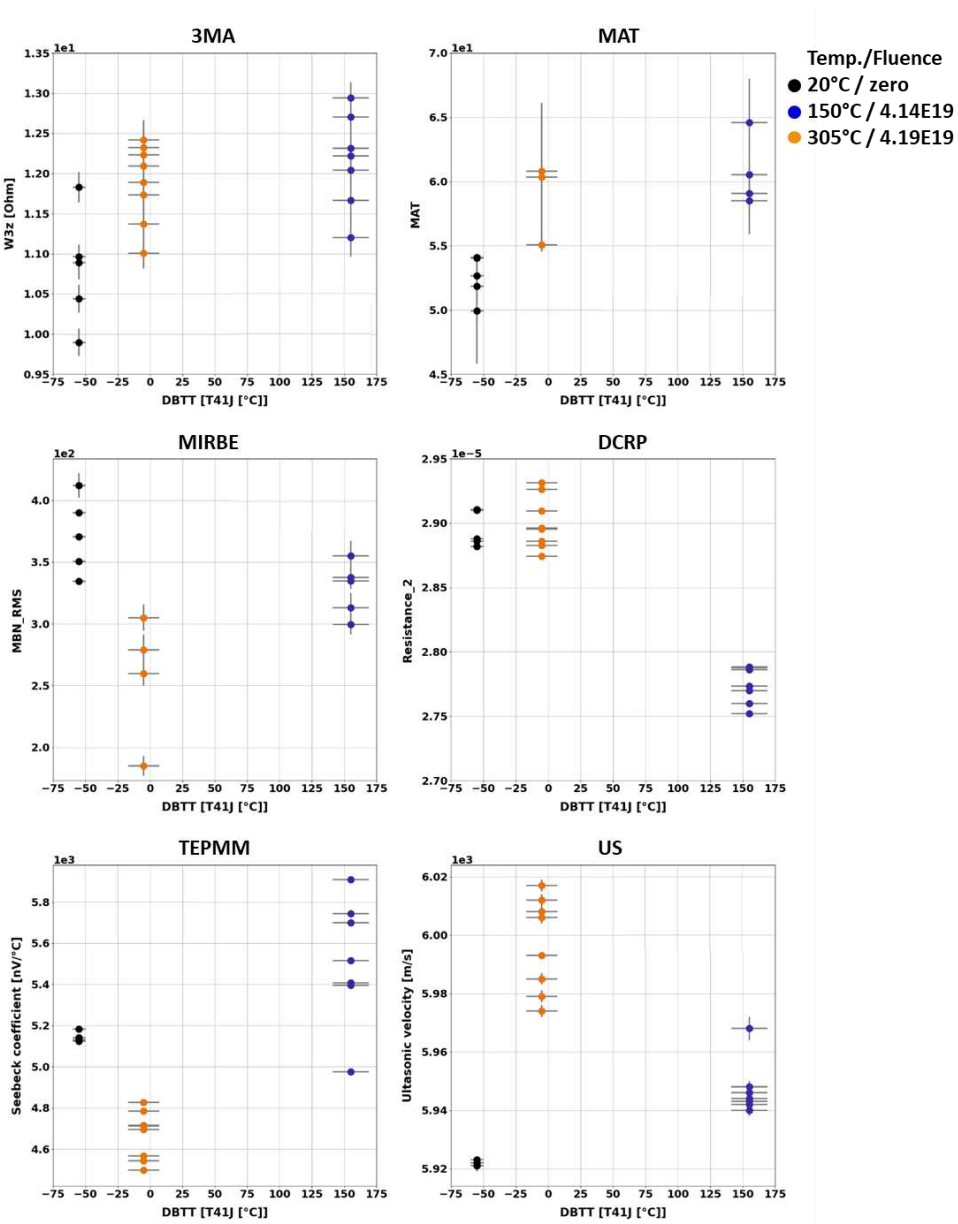

Figure 5. NDE features measured on Charpy samples of A508-B.

Preprints (www.preprints.org) | NOT PEER-REVIEWED | Posted: 14 December 2023 doi:10.20944/preprints202312.1008.v1

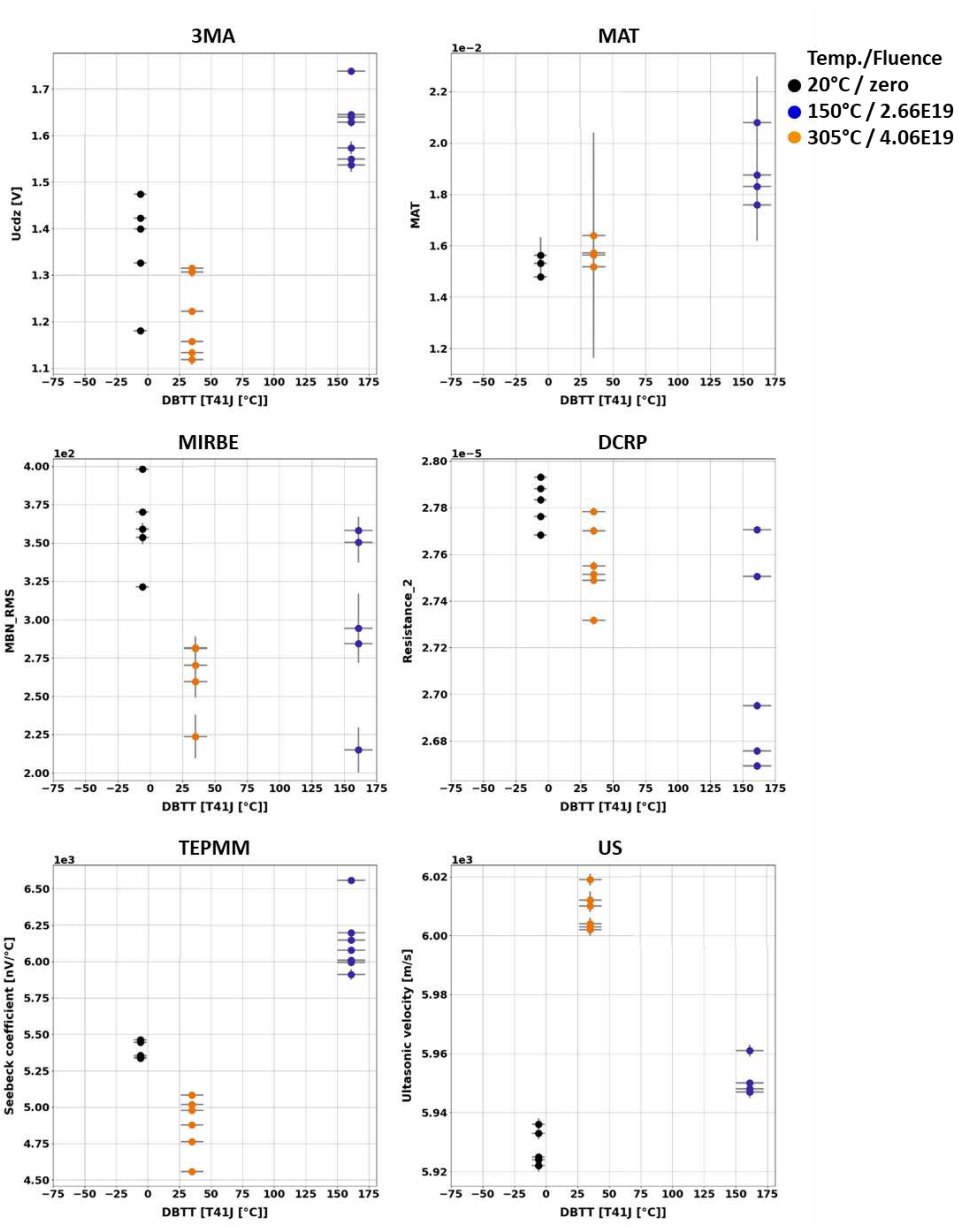

Figure 6. NDE features measured on Charpy samples of HSST-03.

Preprints (www.preprints.org) | NOT PEER-REVIEWED | Posted: 14 December 2023 doi:10.20944/preprints202312.1008.v1

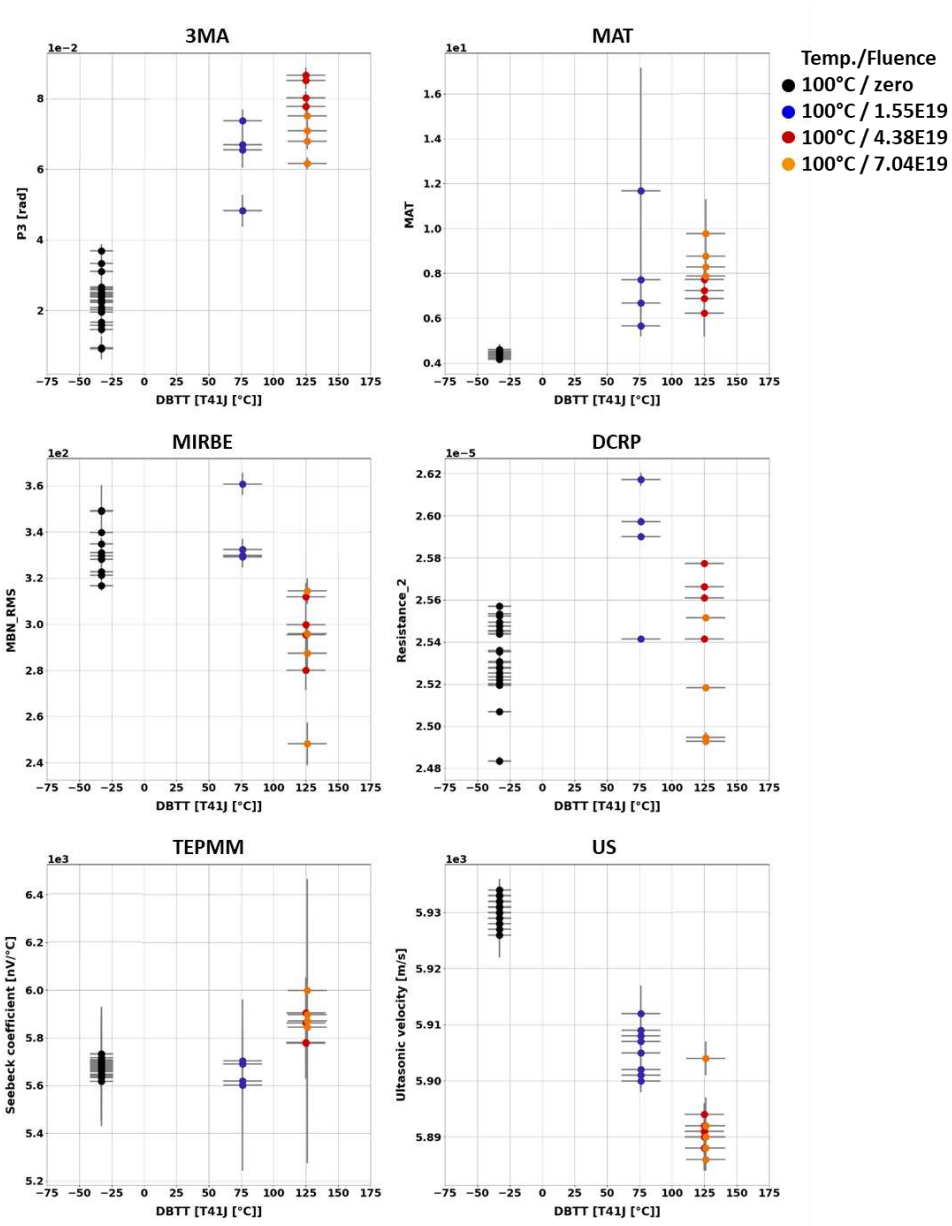

Figure 7. NDE features measured on Charpy samples of A508 Cl.2.

Preprints (www.preprints.org) | NOT PEER-REVIEWED | Posted: 14 December 2023 doi:10.20944/preprints202312.1008.v1

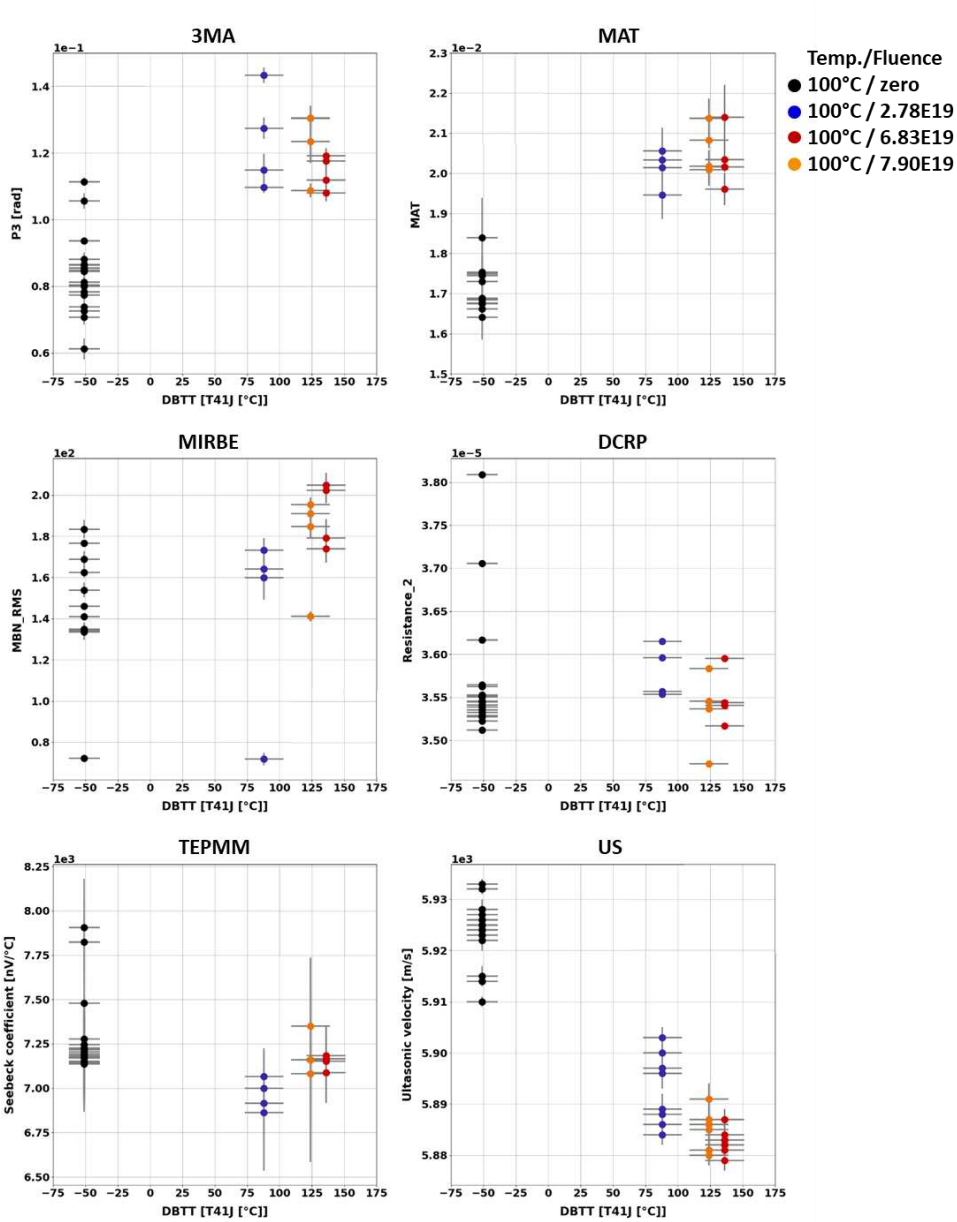

Figure 8. NDE features measured on Charpy samples of 15kH2NMFA.

In case of the material 22NiMoCr37 (irradiated between fluences of $3x10^{19}$n cm^{-2} and $6x10^{19}$ n cm^{-2}) only the Seebeck coefficient continuously changed with increasing DBTT. No difference in terms of the other NDE parameters has been observed for both irradiated conditions (Figure 3). The variation of the DBTT due to increasing fluence taking into account the scatter of points of the 95% confidence bounds of the Charpy test results can't be detected accurately probably due to variations in the microstructure of the material before irradiation.

In case of the weld material 18MND5-W (Figure 4) several NDE features show continuous trends. However, in case of this material the ultrasonic time-of-flight (TOF) of the samples irradiated at 150°C is comparable with the TOF of the non-irradiated samples.

In case of the materials A508-B (Figure 5) and HSST03 (Figure 6) the high irradiation temperature of 305°C affects the outcome of the NDE measurements. Especially the results of the methods MIRBE, Piezo-US and TEPM show an anomalous behavior compared with the other irradiation conditions.

The NDE measurements on the Charpy sample sets of RPV materials of A508Cl.2 (Figure 7) and 15kH2NMFA (Figure 8) investigated before and after irradiation allowed for the first time the characterization of progressive change of embrittlement taking into account the initial condition of the materials (before irradiation). In case of these set of samples it has been observed that the

Preprints (www.preprints.org) | NOT PEER-REVIEWED | Posted: 14 December 2023 doi:10.20944/preprints202312.1008.v1

scattering of outcome of the individual NDE measurements performed on different Charpy samples of the same material and the same irradiation condition is lower.

The influences of the neutron irradiation on several NDE parameters of Charpy specimens have been previously published and discussed in detail [100,101].

8.2.2. Cladded and non-cladded blocks

One of the challenging task of the NOMAD project was to develop a method that can follow the degradation of the base material through the cladding, i.e. the probe can be applied from the inside of the reactor vessel wall. This task raises two problems simultaneously: on one hand to find a way to excite the base material through the cladding, and also to detect the response through the same. On the other hand, the degradation of the base material has to be differentiated from the changes of the cladding properties due to the irradiation.

To decide whether the ferromagnetic base material can be investigated through the austenitic cladding by magnetic methods using an attached magnetizing yoke, numerical simulation of magnetic field was performed to show, how the magnetic field, generated by the magnetizing yoke penetrates into the base material through cladding [102]. The result of this simulation is presented in Figure 9. The result of numerical simulation revealed that by using the large magnetizing yoke for generating exciting magnetic field, the base material could be magnetized sufficiently even through the cladding. On the other hand, when a yoke of a small-sized compared to the thickness of the cladding is applied, it can excite the region of cladding mostly, and the density of the penetrating exciting field in the base material is very limited, almost negligible. This way the cladded system and the cladding only can be studied separately.

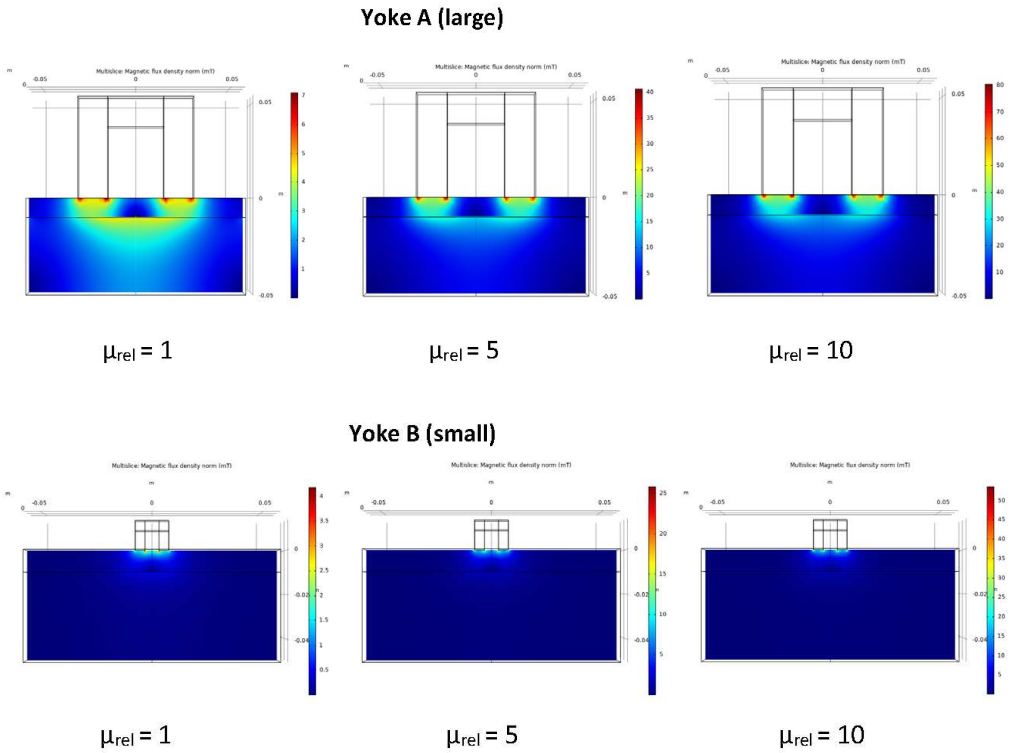

Figure 9. Calculated distribution of the magnetic flux density in a cladded block excited through the cladding when large and small yokes is placed onto the top of the cladding has different relative permeability [102].

To characterize the neutron irradiation induced embrittlement independent of the initial microstructure that can be heterogeneous all blocks have been non-destructively investigated by means of all previously optimized NDE methods before and after neutron irradiation. Some NDE

Preprints (www.preprints.org) | NOT PEER-REVIEWED | Posted: 14 December 2023 doi:10.20944/preprints202312.1008.v1

methods (DCRP and EMAT) are not suitable for the materials characterization through the austenitic cladding.

NDE measurements carried out before neutron irradiation have shown that, similar to the Charpy samples made of the same material, the blocks (non-cladded or cladded) have different material properties. The explanation therefore lies in the different microstructure at different positions in the component where these investigated blocks originate from.

After irradiation, NDE measurements have been carried out again on all non-cladded and cladded blocks. Measuring quantities derived from the NDE methods have been individually collected and analyzed in terms of DBTT. Trends of the non-destructively determined measuring quantities have been identified. An overview of the results obtained on the block samples is given below (Figures 10 and 11).

The influences of the neutron irradiation on MAT parameters of blocks specimens have been previously published and discussed in detail [103,104].

The results of the individual NDE methods have shown the difficulty to characterize the embrittlement by using single-parameter methods.

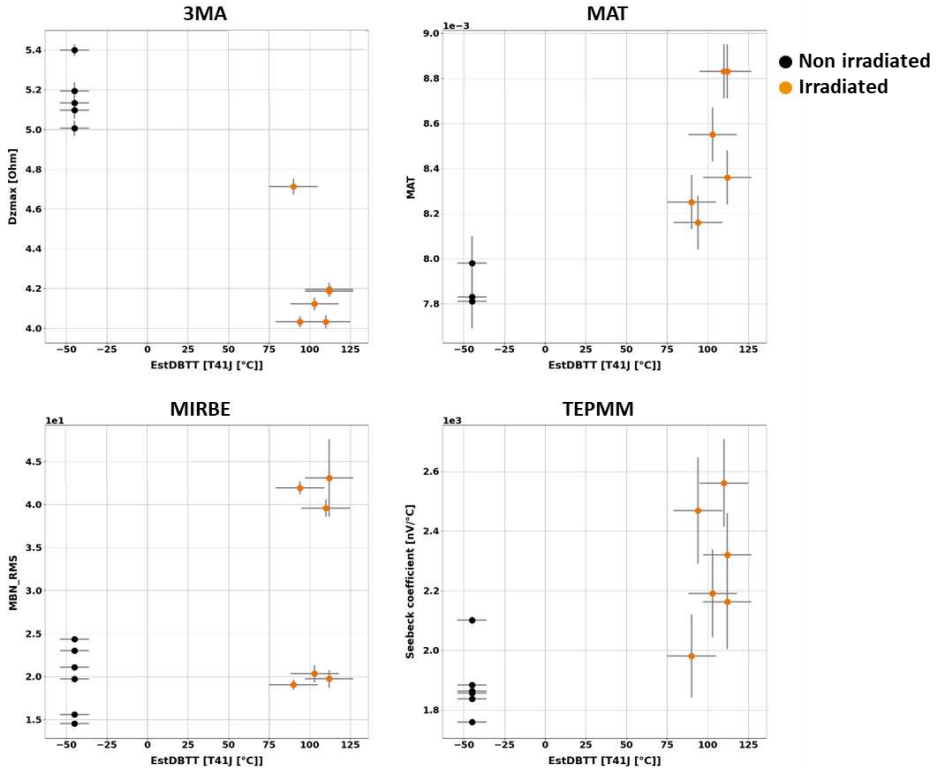

Figure 10. NDE features measured on cladded blocks through the cladding.

Preprints (www.preprints.org) | NOT PEER-REVIEWED | Posted: 14 December 2023 doi:10.20944/preprints202312.1008.v1

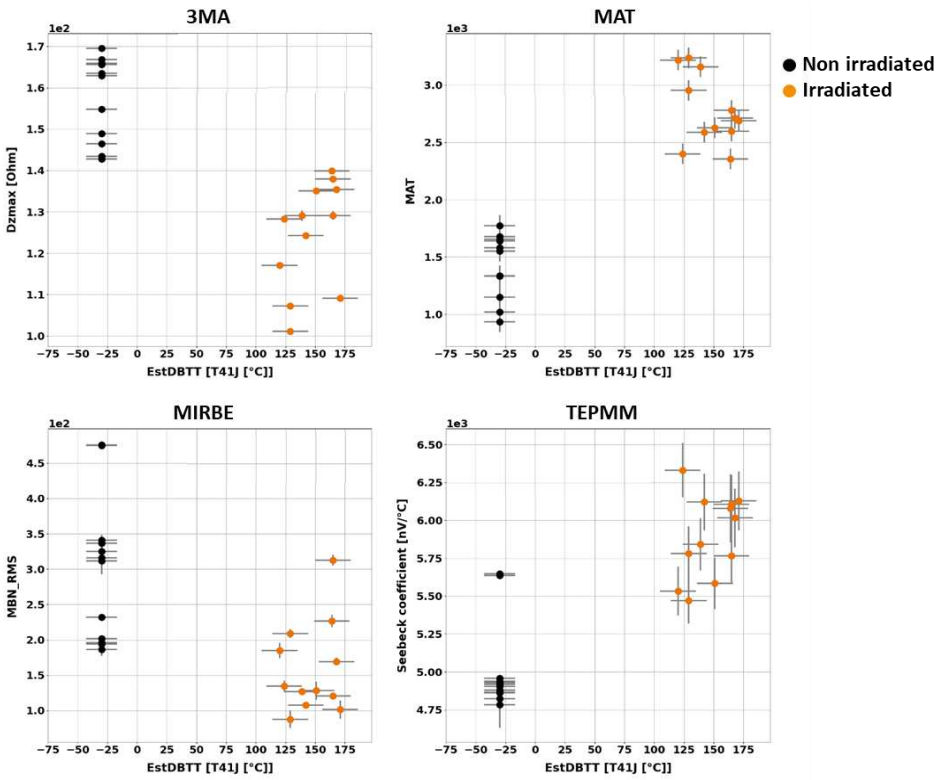

Figure 11. NDE features measured on non-cladded blocks A508 Cl.2 on two opposite sides.

9. Results for prediction of embrittlement by means of a multi-parameter machine learning (ML)-driven approach

9.1. Multiparameter method

Since the individual test quantities have differently weighted sensitivities to target and disturbance quantities, the influence of the disturbance quantities can be eliminated or at least reduced by combining several features that have the potential to suppress overlapped disturbance influences. The advantages of combining test quantities in a multiparameter method are manifold. Such a combination of methods is particularly indispensable when the target quantities, so called independent parameters are to be measured (e.g. DBTT) and the disturbance quantities (temperature, residual stresses, surface condition) can vary simultaneously. The ultimate goal was to produce a machine learning-based computational tool that can estimate the neutron irradiation-induced embrittlement of reactor pressure vessel steel alloys based on the NDE parameters.

In case of multi-parameter, i.e. multi-dimensional nonlinear problems the required analytical expression cannot be formulated typically, so another statistical approach is required. ML algorithms are powerful tools that can be used to automatically create a regression model based on given data. The data must consist of one or several features, which are the input to the model, and one or several target variables, which are the desired prediction of the independent parameters, or in other words, the output of the model.

Since the analytical expression that links the input and the output parameters are not known in case of ML, the transparency is essential for the application of ML, especially in safety areas. Extra attention has to paid to careful studies of these methods and to their verification. In typical supervised machine learning, the model learns from a given training data, and traditionally, a separate validation data set is used to evaluate the performance of the trained model. But here, an additional data set is required for testing the reliability of the method. This set comprises not only some randomly selected elements, but data selected also from the interval boundaries (See in Figure 12). When test result is unsatisfactory, the whole procedure has to be restarted (i.e. “Back to square 1”), by experimenting with new model structure and hyperparameters.

Preprints (www.preprints.org) | NOT PEER-REVIEWED | Posted: 14 December 2023 doi:10.20944/preprints202312.1008.v1

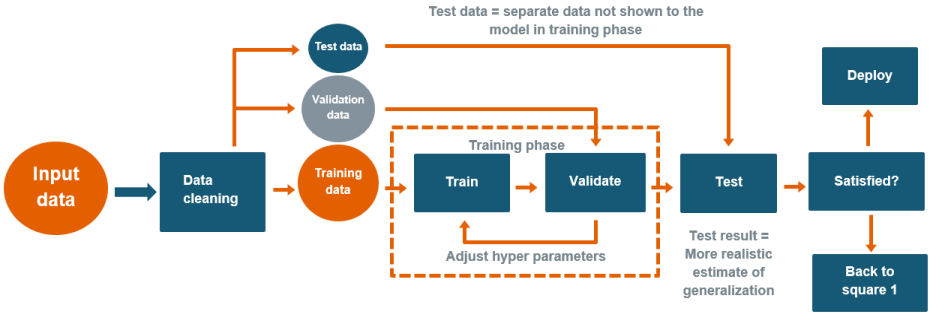

Figure 12. Possible workflow of the ML method application [105].

9.2. Database preparation

Statistical methods work well on a large data set. This raises a quite frequent problem of ML applications: the insufficient number of the achievable measured samples or experimental data, i.e. the limited size of the true result database. The ML methods do not generate any novel information. Instead, they can be used to circumscribe and recognize the information that can be found in the database. Pre-processing the obtained database of the physical test results aims to ease this task of the ML approach and increases its performance, i.e. increases the precision of the regression or classification. Any operation on the experimental data set should be carried out with special attention not to degrade the targeted information content or falsify it.

There are basically two options for processing the database: eliminating some of its elements considered as useless ones, and modifying its entries, or even generating novel ones in an artificial way.

9.2.1 Reduction of input space dimension

If the analysis includes too many features that have a weak correlation with the target variable, they can reduce computational efficiency, increase model complexity, and make it harder to interpret. Moreover, increased model com-plexity results in a higher probability of overfitting. A large number of features prompts a problem known as the curse of dimensionality: when the number of dimensions increases, the volume of the feature space increases, and the data becomes sparser. As the number of features increases, the number of samples required to maintain accuracy grows exponentially [105].

One of the most evident methods for reducing the dimension of the input space is to remove the least relevant features (i.e. input parameters). This reduces the complexity of the ML algorithm's problem. There are various simple statistical evaluations or more complex regression methods to study the importance of the different features.

9.2.2. Determining feature importance

As an example, the Wilcoxon signed-rank test [106] can be used to study the statistical significance of materials properties caused by the irradiation in this paired data set. This test calculates the synthetic parameter differences for each pair of measurements and separately for each NDE feature. The outcome of the test is the p-value for the null hypothesis that the difference has a zero expectation value and a symmetric distribution. This corresponds to the conclusion that the irradiation did not affect the feature. The p-value is compared to a predefined significance level: If the p-value is greater than the significance level (threshold), the null hypothesis is accepted and we conclude that the irradiation has not caused a change in the feature, which can then be excluded from the analysis.

In the NOMAD project, the analysis focused on identifying which NDE parameters out of the 28 available contribute to precision and can aid in recognizing and suppressing side effects. In addition, the project isolated the parameters that are irrelevant and have no impact. Different types of ML algorithms tested in competition and their performances have been evaluated (see the example in Figure13).

Preprints (www.preprints.org) | NOT PEER-REVIEWED | Posted: 14 December 2023 doi:10.20944/preprints202312.1008.v1

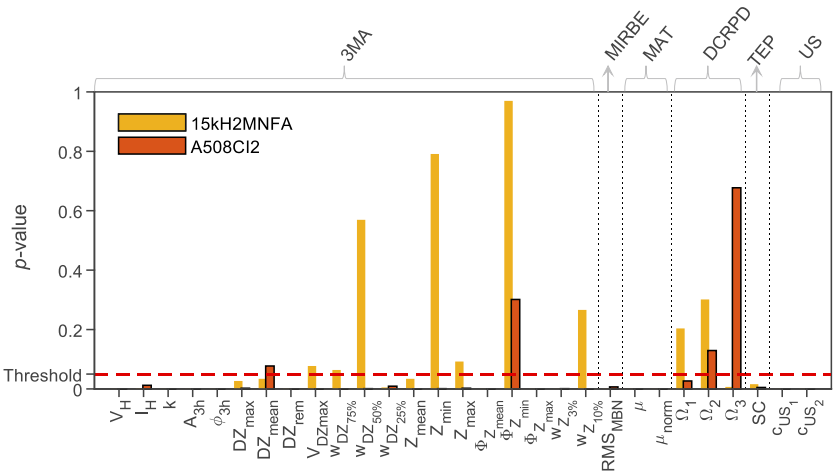

Figure 13. Example: Wilcoxon test results obtained on 29 NDE features (i.e. measurement output parameters) of the NOMAD project [105].

Wilcoxon signed-rank test is a simple approach that can be applied even on very limited dataset but also with limited accuracy. However, when the dimension of the database allows it, even more sophisticated methods can be implemented to study the importance of the input features. Ensembles of decision trees can be used for this purpose. The boosted decision tree (BDT) algorithm and the extra-trees regressor (ETR) algorithm can be used for better evaluation of the different feature significance (see in Figure 14). These methods are typically not for the primary assessment, but rather for optimizing the ML tool to be developed [104].

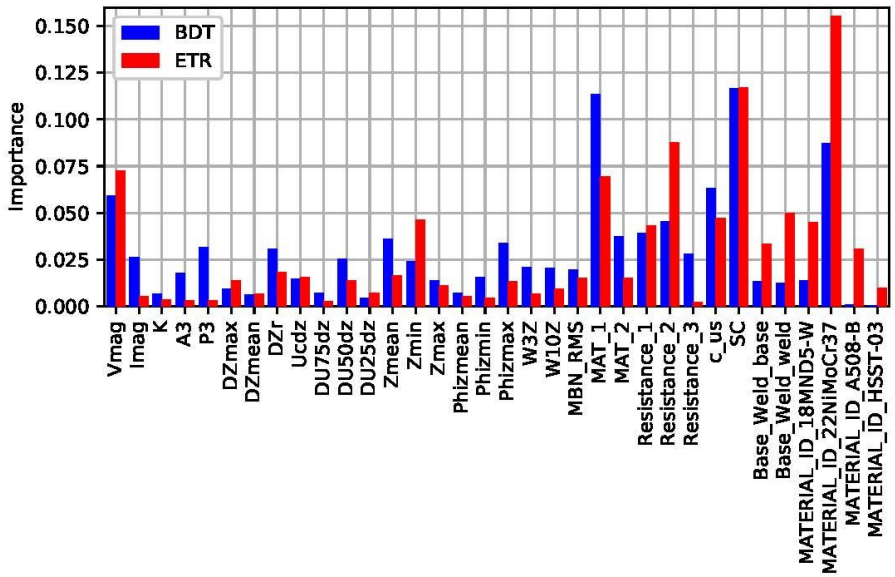

Figure 14. Example: The relative **importance** of the features evaluated by the models built with the boosted decision tree (BDT) algorithm and the extra-trees regressor (ETR) algorithm plotted as bar plots in case of NOMAD database involving six different tested materials [104].

9.2.3. K-fold cross-validation score

A traditional method to train a machine learning model is to set aside a third data set from the training data, known as testing data set that is used to test the different hyperparameter combinations (i.e. the combinations of those external configuration variables used to manage machine learning model training), for example. However, the model can be also trained using *k*-fold cross-validation [107], where the training set is divided into *k* parts, known as folds, and then one by one, each fold is

 doi:10.20944/preprints202312.1008.v1

used as a so-called test, or validation, set while the other $k-1$ folds are used to train the model. This is repeated k times and an averaged cross-validation score is calculated based on the predictions. Obviously, the separate test set must still exist and should be held out of this training process. There are several benefits to cross-validation: the real test set is not shown to the model at any point of the training process, and the k-fold cross-validation score provides an estimate of the test accuracy of the model.

The k-fold score is used to fine-tune the data pre-processing steps and the hyperparameters of the model. But it can also be used for determining the less relevant parameters. Dropping one of the features reduces the dimensionality of the feature space and can improve the performance of some algorithms. This way, dropping one by one the one-hot encoded features and calculating the k-fold cross-validation score for each feature, the least significant features can be identified and eliminated from the database [108].

9.3. Manipulating the database

In order to increase the achievable classification accuracy of the ML methods, the quality of the otherwise limited database can be improved by manipulating its content. Artificial manipulation of any data obtained from real, i.e. physical experiments sounds surprising at first, since this involves significant risks of falsification and of losing the transparency of the ML method application.

It is quite typical when multiple different measurement principles are utilized for obtaining multidimensional response on the tested target, that some of measurement parameters become invalid in certain measurement cases. Here, invalid means that the related method cannot be applied in the given circumstances or some of the NDE probes fail because of a side effect occurring. As a consequence, the aggregated database will be not only limited due to the limited availability of test cases, but it will also be incomplete: there will be missing elements or existing elements having invalid values in it. Either the missing elements or the invalid elements degrade the classification accuracy.

9.3.1 Cleaning the database

Database cleaning covers the efforts on identification and marking or eliminating database elements that can be recognized as undoubtedly false or missing before the database is used for training the ML methods. This step is not only an option but rather a necessary step in the practice.

The missing elements, as well as the invalid elements can be marked in the same way and both types can be considered as holding no information. One of the possibilities in practice is to substitute these values with a special number value, that is defined exactly for this purpose: NaN (i.e. Not a Number) [104]. This way the database becomes uniform and suitable for further processing in terms of meaning that all of its elements will contain uniformly encoded elements. Inserting or replacing elements to NaNs in the database does not alter the information it holds, but this makes possible to work on it with standard algorithms and software codes.

9.3.2 Dealing with NaNs

By having NaNs in the database further steps are available for improving the database for ML. If the elements of a certain test case contain too many NaNs or several of its significant elements are NaNs, such test cases (i.e. database rows) can be eliminated completely from the database since they cannot contribute to training the ML methods. Obviously, if all the measurement cases are deleted, where at least one parameter is missing (so called listwise deletion) it does not cause any bias in the prediction of the ML methods, but dramatically degrades the power of the classification. Therefore, the listwise deletion cannot be applied practically where the database is rather limited.

Instead of deletion, there are also different methods of predicting the missing values by either considering the statistics of its available neighbors, when possible, or filling them automatically by algorithms even by the help of ML techniques that consider global features not local ones.

9.3.3. Data augmentation and imputation

Preprints (www.preprints.org) | NOT PEER-REVIEWED | Posted: 14 December 2023 doi:10.20944/preprints202312.1008.v1

The aim of both the data augmentation and the imputation is to increase the classification accuracy [109]. Obviously, extending the database of the measured data with "artificially generated" values involves the possibility of either falsification or it can establish a "positive" feedback that can lead to miss prediction or misclassification at the end. The database extension has relevance primarily for the training of ML algorithms. This way the unwanted side effect of the database manipulation can be caught by testing the algorithm that was trained on the extended database and on the database without any extension.

9.4 Using ML methods

In the NOMAD project, following the database pre-processing, the training data was used to train three models: Huber loss regression (HLR) [110], support vector regression (SVR) [111] and an artificial neural network (ANN) [112]. In order to compare the performance of these three methods, the 10-fold cross-validation score is measured as the mean absolute error (MAE). Both test and training scores are reported as MAE, root mean square error (RMSE) and R^2 i.e. coefficient of determination score. Table 6 summarizes the result of this study:

Table 6. The 10-fold cross-validation, training and test scores of the three models [107].

		HLR	SVR	ANN
10-fold cross-validation score	MAE [°C]	13.67	13.58	12.7
Training score	MAE [°C]	9.32	8.68	9.21
	RMSE [°C]	14.49	13.63	12.57
	R^2	0.97	0.97	0.98
Test score	MAE [°C]	17.1	17.77	16.04
	RMSE [°C]	18.67	20.4	22.08
	R^2	0.95	0.94	0.93

In certain applications of the NOMAD project, +/-25°C DBTT shift had to be detected. All of these three methods could provide significantly better prediction of the DBTT shift than this error threshold. It can be also deducted, that practically all three methods reached similar performance, i.e. the test scores vary 16…18 °C. The most complex approach, the ANN could also perform very well, despite the extraordinarily limited dataset.

Since the ANN requires the largest computational power, this test resulted in the SVR prevailing, as this method provides the optimal balance between the classification accuracy and the required computational power. Certainly, this claim is valid only for the given NOMAD database.

9.5. Results of NOMAD ML approach

Within the framework of the NOMAD project, an SVR method was used to create models that accurately predict the neutron irradiation-induced embrittlement, measured as the DBTT, even though the data set is small. The SVR is a supervised machine learning algorithm that relies on kernel functions to solve problems that cannot be handled directly by linear classification. The SVR is flexible enough that it provides robust results even though the number of data points is low, and it is considerably simpler to optimize than other, e.g., neural network algorithms [104]. To evaluate the performance of the trained models in predicting the neutron irradiation-induced embrittlement of steel alloys based on non-destructive measurements two different model evaluation metrics were used.

9.5.1 Test score in NOMAD

The traditional method to analyze the generalization skill of a machine learning model is to split the data set into training and test sets. The model is trained entirely based on the training set, and when the model has been fully trained, the generalization skill of the model is tested using the test

Preprints (www.preprints.org) | NOT PEER-REVIEWED | Posted: 14 December 2023 doi:10.20944/preprints202312.1008.v1

set by feeding it to the model without its target values. After the test set has been shown to the model, the model should not be modified to produce an improved test result. The training process refers to the optimization of the model hyperparameters, and most of the time it also includes pre-processing steps, such as the selection of the feature scaling scheme. The trained model makes predictions based on the test set features and the predictions of the independent parameters are compared to the true target values of the test set. The test and training sets must be equally representative of the whole data set; otherwise, the test score does not represent the generalization skill of the model with the best accuracy. Commonly, the test set is a random subset of the whole data set, with a size of 20% of the size of the whole data set. The rest, 80% of the data then constitutes to the training set (this procedure is referred to as the 80/20 split). The larger and more diverse the training data set is, the more flexible and accurate the model will yield.

Three models were generated for the prediction of the embrittlement: one based on data obtained on Charpy specimens only, one based on data obtained on Blocks only and one based on mixed data obtained on Charpy and block specimens. The models to predict DBTT are based on supervised ML using the SVR model implemented in scikit learn and were trained and tested using the database. The database contains different materials which are marked by one-hot Boolean values in both the database and the tool. The input data is prepared using the Min/Max Scaler function within scikit learn.

The results obtained for the three different models are summarized in Table 7. The table presents the cross-validation scores of the fine-tuned models, the training scores, and the test scores. As can be seen from the results, all test MAEs are under 19 °C and the test R2 scores are equal or greater than 0.9. The accuracies of the models are also visualized in form of correlation plots in Figures 15-17, where the predictions made by a model are plotted as a function of the DBTT values *determined with Charpy tests.*

Table 7. A summary of the accuracies of the models. The number of folds *k*, *k*-fold cross-validation scores, training scores and test scores are reported for each model. The scores are reported as mean absolute errors (MAEs), root-mean-square errors (RMSEs) and R^2 scores.

Data set	*k*	*k*-fold MAE [°C]	*k*-fold R^2	Train RMSE [°C]	Train MAE [°C]	Train R^2	Test RMSE [°C]	Test MAE [°C]	Test R^2
Charpy of all RPV steels	10	13.17	-	7.26	6.59	0.99	23.69	15.95	0.92
Blocks: test/train	38	11.58	-	4.99	4.06	1.0	22.17	17.8	0.93
All samples of A508 Cl2	10	13.02	-	8.18	5.79	0.99	17.56	13.47	0.96
Charpy + blocks: 50/50	10	25.68	-	13.1	8.02	0.98	26.21	18.65	0.9

Preprints (www.preprints.org) | NOT PEER-REVIEWED | Posted: 14 December 2023 doi:10.20944/preprints202312.1008.v1

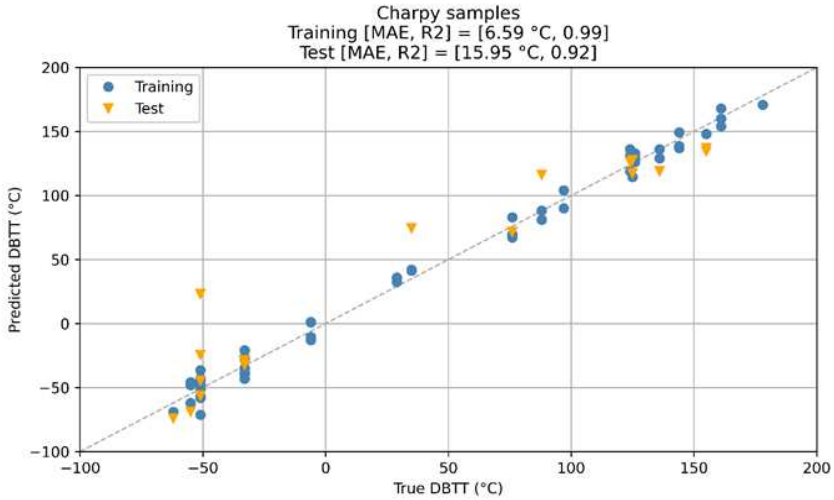

Figure 15. The correlation plot for the Charpy samples. The true values of the ductile-to-brittle transition temperature (DBTT) are plotted on the x-axis, and the predictions made by the SVR model are plotted on the y-axis. Samples in the training set are plotted as steel blue dots, and samples in the test set are plotted as orange triangles. The grey diagonal line represents a perfect fit. The training and test scores, measured as the mean absolute error (MAE) and R^2 score are reported in the heading.

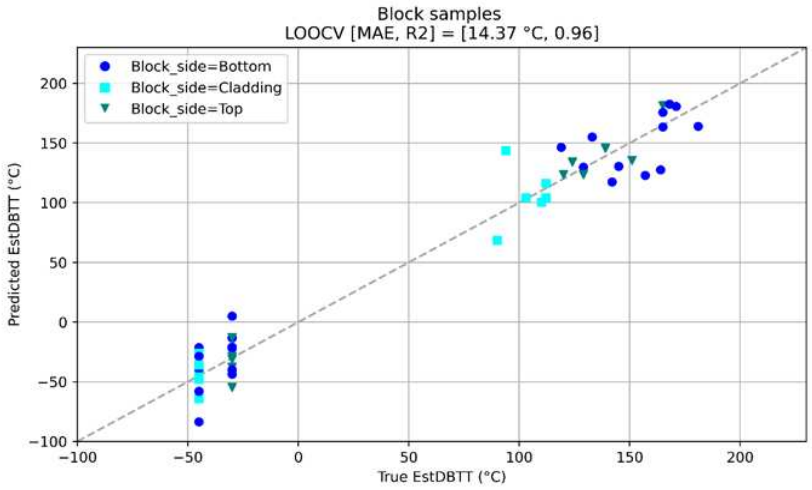

Figure 16. The leave-one-out cross-validation procedure results performed on the entire block data set, which contains 48 samples. The true values of the estimated ductile-to-brittle transition temperature (EstDBTT) are plotted on the x-axis, and the predictions made by the SVR model are plotted on the y-axis. The measurements taken from different block sides, top, bottom and through the cladding have been plotted with different colours and shapes. The LOOCV mean absolute error (MAE) and R^2 score are reported in the figure heading.

Preprints (www.preprints.org) | NOT PEER-REVIEWED | Posted: 14 December 2023 doi:10.20944/preprints202312.1008.v1

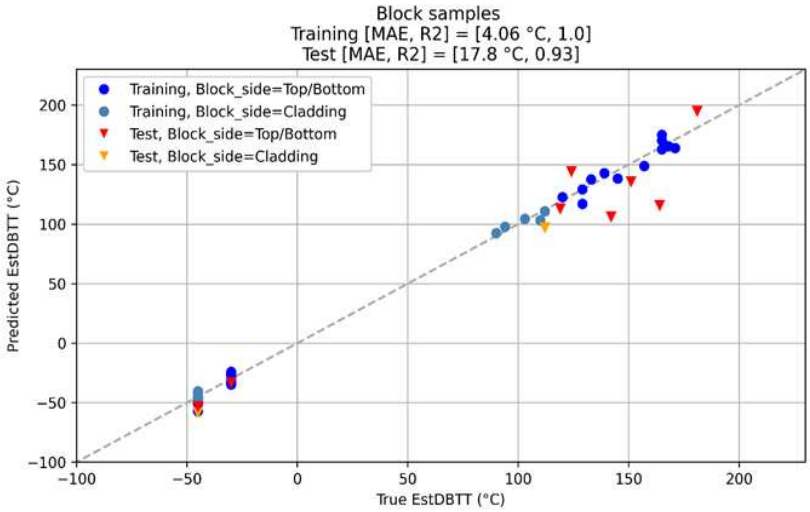

Figure 17. The correlation plot for the block samples. The true values of the estimated ductile-to-brittle transition temperature (EstDBTT) are plotted on the x-axis, and the predictions made by the SVR model are plotted on the y-axis. Samples in the training set are plotted as blue/steel blue dots, and samples in the test set are plotted as orange/red triangles. Whether the measurement was made through the cladding or not is indicated by the colours. The grey diagonal line represents a perfect fit. The training and test scores, measured as the mean absolute error (MAE) and R^2 score, are reported in the heading.

While the NOMAD study has been conducted on different sample types, including large cladded blocks, the validation focuses on data collected on Charpy samples only due to the limited number of samples available for uncladded and cladded blocks. A transfer of the findings to block types is per se not possible and would require a new validation respectively. Hence, the validation process is a proof-of-concept regarding the Charpy samples. The validation has been established by a detailed evaluation of the functionality of the NOMAD tool. This has been done in the context of the regression as well as it has been complemented by a classification approach too.

In addition to the train and test data set, a validation data set is introduced for the tool validation. The validation set remains constant throughout the entire validation process and is not considered for training nor testing. This ensures that the different validation procedures can always be compared through the same validation set. The validation data set consists of 9 samples and contains only measured NDE values (no data augmentation is used in the validation set).

The robustness of the NOMAD tool was challenged by splitting the test and train set in a way that one temperature level was used for the test set and thus was entirely left out for training. Temperature levels used for testing were 124°C-126°C. This analysis gives insight to the question whether the algorithm is overfitted as well as to its ability to interpolate between different temperature levels. The results are shown in Figure 17. The results show that the NOMAD tool still performs very well, and very good performance metrics are achieved even if one temperature level is not included for training.

Preprints (www.preprints.org) | NOT PEER-REVIEWED | Posted: 14 December 2023 doi:10.20944/preprints202312.1008.v1

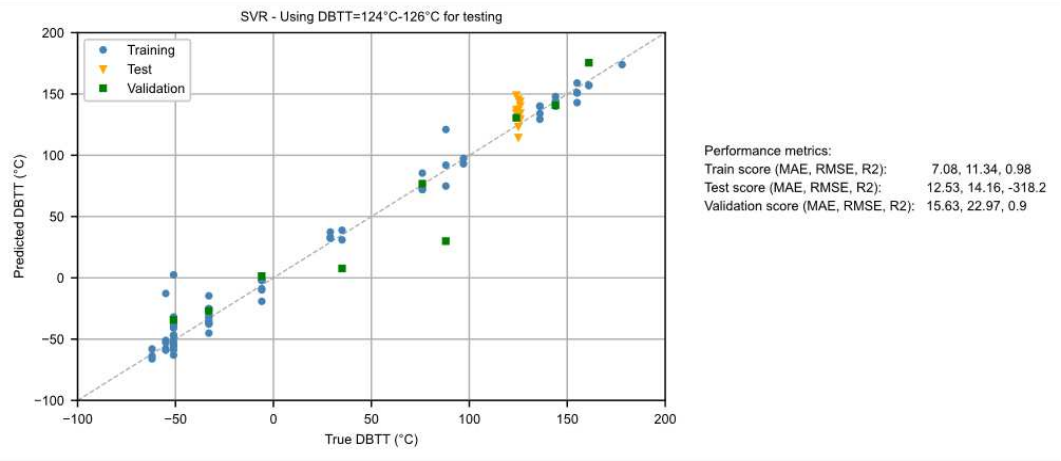

Figure 17. NOMAD tool performance evaluation leaving out the temperature level around 125°C for training (orange markers).

10. Discussion

A total of nearly 200 non-irradiated and irradiated samples were provided, mechanically tested, non-destructively measured and the results evaluated and analyzed.

The sample set was consisting of Charpy samples of six different materials and of block shaped samples of one material, whereby a part of the block samples was covered with the cladding in order to simulate the real pressure vessel situation. In total 28 NDE parameters out of six NDE methods (three magnetic, electric, thermal and ultrasonic methods) were measured from all provided samples. In parallel, the various specimens were tested destructively to determine the irradiation induced changing in their properties, including tensile, Vickers hardness and Charpy impact transition curves allowing the determination of the DBTT.

Previously to the NOMAD project none of the NDE methods or their output parameters could reach the required precision and reliability for application in determining the DBTT.

It can be noticed, that samples within one material and degradation group show a large variation in the measured feature. This may be caused by influences overlapped to the DBTT caused for example by material inhomogeneity's, machining variation or variation in the surface condition. Single features are not suitable for the determination of DBTT. However, a combination of several features may have the potential to suppress these overlapped disturbance influences. A possible interpretation of the large scatter of measured points is given in Appendix B.

The advantages of combining test quantities in a multiparameter method are manifold. Such a combination of methods is particularly indispensable when the target quantities to be measured (e.g. DBTT) and the disturbance quantities (temperature, residual stresses, surface condition) can vary simultaneously. Since the individual test quantities have differently weighted sensitivities to target and disturbance quantities, the influence of the disturbance quantities can be eliminated or at least reduced in this way.

The NDE methods are a kind of inverse problem solutions that measure not the targeted physical quantity in direct manner but other physical quantities can be linked with, based on physical background. However, the irradiation effects are complex processes inside the material that affect the recorded quantities in different manners.

This is why a stand-alone NDE method based on a single physical principle has to face with the problem of several side effects resulting in unacceptable scattering of the output parameter. Therefore, the basic idea of the NOMAD project is to use multi-method/multi-parameter approach and to focus on their synergies that allows recognizing these side effects and therefore suppressing them, as well.

The nuclear industry already applies several statistical methods where the statistical parameters can be calculated by analytical expression. The Charpy Impact Test itself is an example, where the transition temperature curve is derived from the pool of the measured data by mathematical fitting.

In case of multi-parameter, i.e. multi-dimensional nonlinear problems the required analytical expression cannot be formulated, so other statistical approach is required: the machine learning (ML).

Since the analytical expression that links the input and the output parameters is not known in case of ML, the transparency is essential for the application of ML, especially in safety areas. We paid large attention to careful studies of these methods and to their validation. We have analyzed separately, which NDE parameters (out of the 28) can contribute to the precision or can help the algorithm to recognize and suppress the side effects and which ones are irrelevant and can be left out without any effect. Different types of ML algorithms tested in competition and their performances have been evaluated. Unfortunately, the details of this extensive study are far beyond this paper.

The important outcome of the ML technique is that not only one, but several different ML techniques could reach required precision and reliability, i.e. to keep the DBTT prediction error lower than +/-25°C, which was previously not possible at all for each individual NDE method independently.

Although many specimens were investigated within the framework of the NOMAD project, the gathered database is extraordinary limited from ML point of view. Statistical methods work well on large data set. This raises a quite frequent problem of ML applications: the insufficient number of the achievable measurement samples or experimental data, i.e. the limited size of the result database. The task of ML methods is to circumscribe and recognize the information that can be found already in the database.

In order to ease this task, different ways of pre-processing the database are studied in order to increase the precision of the classification. The dimension of the database was reduced by eliminating features having no significant importance, i.e. dropping those measurement outputs cannot contribute to the classification performance. Different methods can be applied for this feature selection, starting with simple statistical approach (like the Wilcoxon signed-rank test) but also more complex ones like the different ensembles of decision trees. The K-fold cross-validation technique can also be used for scoring the different inputs and for optimizing the database. The database cleaning means not only the elimination of the unusable input parameters, but it covers also the possibilities of the data augmentation and imputation. The aim is clear: to provide better dataset for training of ML algorithms without falsifying or biasing the dataset. However, every step of data manipulation should be transparent, otherwise the technique cannot be accepted in safety critical areas.

The present results of the individual NDE measurements together with the ML evaluation proved their suitability to characterize the degradation of reactor pressure vessel steels caused by a simulated operation condition. A calibration/training procedure was carried out on the merged outcome of testing methods with excellent results to predict transition temperature, yield strength and mechanical hardness for all investigated materials.

The estimation of radiation damage of a reactor vessel through the cladding is a very challenging problem. Experimental and numerical studies have been carried out to analyze how the base material can be excited through the cladding and how the properties of the cladding and base material, thus their changes, due to the irradiation can be separated. These results have been published already in the case of MAT method [102-104].

The results can be useful for the future potential introduction of this (and in general, any) nondestructive evolution method.

11. Summary and conclusions

The large test program was successfully completed. A total of more than 700 samples were mechanically tested and analysed. The various steps of preparation, support and execution of the multiple hot-cell campaigns allowed the NDE partners to investigate several hundreds of irradiated samples. As a result, 28 NDE parameters were measured on a variety of materials, specimens and irradiation conditions. In parallel, the various irradiated specimens were tested destructively to determine the post-irradiation properties, including tensile, Vickers hardness and Charpy impact transition curves allowing the determination of the DBTT.

 doi:10.20944/preprints202312.1008.v1

Previously to the NOMAD project none of the NDE methods or their output parameters could reach the precision and reliability are required for application in determining the DBTT. The irradiation results in complex processes inside the material that affect the recorded quantities in different ways. This is why a standalone NDE method based on a single physical principle has to face with the problem of several side effects resulting in unacceptable scattering of the output parameter. However, as it is proven in Appendix B, this large scatter is probably due to the originally existing inhomogeneity of the investigated material. This is a very important conclusion of the project: not the possible error of applied magnetic methods is responsible for the scattering of measured parameters.

The basic idea of the NOMAD project is to use multi-method/multi-parameter approach and to focus on their synergies that allows us to recognize these side effects therefore supressing them, at the same time.

The nuclear industry already applies several statistical methods where the statistical parameters can be calculated by analytical expression. The Charpy Impact Test itself is an example, where the transition temperature curve is derived from the pool of the measured data by mathematical fitting. In case of multi-parameter, i.e. multi-dimensional nonlinear problems, the required analytical expression cannot be formulated, so other statistical approach is required: the machine learning (ML).

Since the analytical expression that links the input and the output parameters are not known in case of ML, the transparency is essential for the application of ML, especially in safety areas. We paid large attention to careful studies of these methods and to their validation. We have analysed separately, which NDE parameters (out of the 28) can contribute to the precision or can help the algorithm to recognize and suppress the side effects and which ones are irrelevant and can be left out without any detrimental effect. Different types of ML algorithms have been tested in terms of competition of their performances have been evaluated. Unfortunately, the details of this extensive study is far beyond of this paper.

The important outcome of the ML technique is that not only one, but several different ML techniques could reach required precision and reliability, i.e. to keep the DBTT prediction error lower than +/-20°C, which was not possible at all previously for the single NDE method.

Although hundreds of specimens were investigated within the framework of the NOMAD project, the gathered database is extraordinary limited from ML point of view. So, we can consider our carried out work as a kind of feasibility study. The next step should be to extend the data set. Nevertheless, the present results of the individual micromagnetic measurements together with the ML evaluation proved their suitability to characterize the degradation of reactor pressure vessel steels caused by simulated operation condition. A calibration/training procedure was carried out on the merged outcome of testing methods with excellent results to predict transition temperature, yield strength and mechanical hardness for all investigated materials.

The estimation of radiation damage of a reactor vessel through the cladding is very challenging problem. Experimental and numerical studies have been carried out to analyse how the base material can be excited trough the cladding and how their properties of the cladding and base material, therefore their changes due to the irradiation can be separated. These results have been published already in case of MAT method.

Our results, achieved within NOMAD project can be useful for the future potential introduction of this (and in general, any) nondestructive evolution method.

Acknowledgments: This research was carried out in frame of the "NOMAD" project. This project (Non-destructive Evaluation System for the Inspection of Operation-Induced Material Degradation in Nuclear Power Plants) received funding from the Euratom research and training programme 2014–2018 under grant agreement No 755330.

Appendix A: Description of magnetic NDE methods

1. MAT

Preprints (www.preprints.org) | NOT PEER-REVIEWED | Posted: 14 December 2023 doi:10.20944/preprints202312.1008.v1

A non-destructive testing method, called Magnetic Adaptive Testing (MAT) was developed for detecting different types of degradation of ferromagnetic materials in Centre for Energy Research. This method is an expansion of traditional magnetic hysteresis measurements. In contrast to it, where investigated samples are characterized by their single major hysteresis loop, this method studies the complex set of minor magnetic hysteresis loops of each sample within the investigated series. As presented in the theoretical Preisach hysteresis model [113], the complex sets of minor magnetic hysteresis loops contained a lot of information about the material properties. Physical principles of MAT, experimental applications and method of evaluation of recorded data are described detailed in Ref. [70].

The samples to be measured are magnetized by a magnetizing yoke, which is placed on the surface of the sample. The size of the yoke should be chosen to fit the size of investigated samples. A magnetizing coil and a pick-up are wounded on the bows of the yoke. The yoke is a C shape laminated FeSi transformer core. The current of the magnetizing coil is changed in a triangular shaped time function, by fixed slope and the maximum of amplitudes are gradually increasing by a pre-defined step in each reverse magnetization cycle. The signal induced in the pick-up coil is proportional to the differential permeability of the measured material.

$$\mu(h_a, h_b) = const * U(h_a, h_b) = const * \partial B(h_a, h_{bj}) / \partial h_a * \partial h_a / \partial t$$

where ha(t) is the effective field, produced in the magnetizing circuit and hb is the amplitude of the minor loops. Time variation of magnetizing current and the detected permeability loops are shown in Figure 1. Before measurement the sample is demagnetized by decreasing amplitude magnetizing current, so in each case the measurements start on samples having zero magnetic moment.

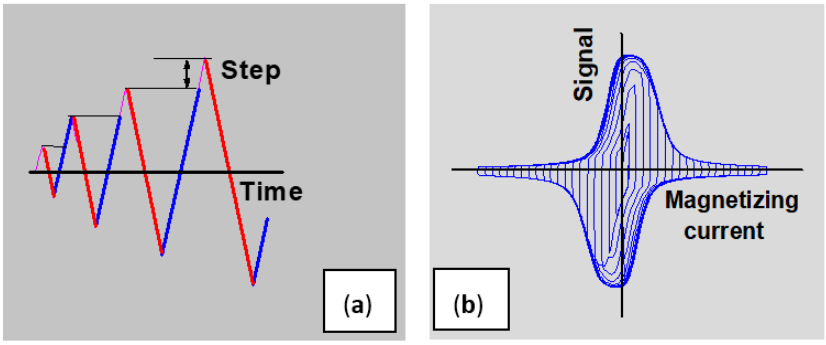

Figure A1. Time variation of magnetizing current (a) and the detected permeability loops (b).

The detected series of minor permeability loops serve as a base of the further evaluation. All sets of hysteresis loops are re-computed into a matrix of elements. These elements are positioned by field coordinates (h_a,h_b). Each matrix element can be used as a magnetic descriptor, which characterizes the structure variation of the investigated sample. As an illustration, the calculated μ(h_a,h_b) permeability matrix is presented in Fig A2. If a series of samples is measured, such a matrix is determined for each sample. This matrix contains a lot of information. Other matrices can also be calculated, e.g. the hysteresis matrix by integration of directly measured permeability values, or first derivative of permeability values. Sometimes these matrices characterize the material degradation better than the permeability matrix.

Preprints (www.preprints.org) | NOT PEER-REVIEWED | Posted: 14 December 2023 doi:10.20944/preprints202312.1008.v1

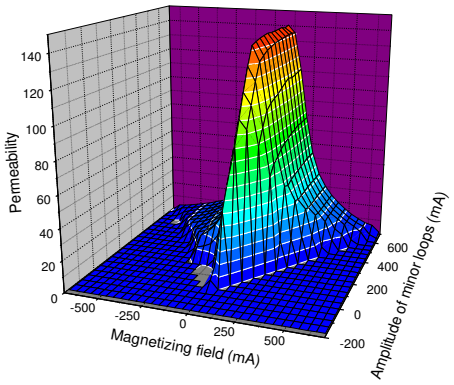

Figure A2. Permeability matrix.

MAT is a comparative method, it does not yield absolute values of magnetic quantities, but it is suitable to follow material changes, due to any external effect. For this purpose, another program of evaluation was developed as well: the actual matrix elements are divided by the corresponding matrix elements of the reference sample in original state. The result is a standardized μ(x) matrix, the elements of which contain all of the information about material degradation, and 'x' is the so called independent parameter, which characterizes, what happened with the investigated material: plastic or elastic deformation, fatigue, neutron irradiation, thermal treatment, etc.

Degradation functions having different coordinates differently react to the studied degradation. A procedure is used, which is able to pick up those descriptors, which react optimally to the considered way of degradation of the investigated material. The optimal, the most sensitive and the most reliable descriptors are used for detecting the structural modifications of the material in question.

The selection of the optimal descriptor increases the reliability and the robustness of this method. It is also possible, to analyze the know 'side effects' of the certain application and to identify those descriptors are mainly affected by these disturbances. This way an opportunity can be established for suppressing measurement uncertainties that can improve the method robustness further.

A careful analysis of potential experimental errors was performed in Ref. [114] and it was found that by taking into account of all possible sources of uncertainty, the error of the whole MAT evaluation is less than 1%.

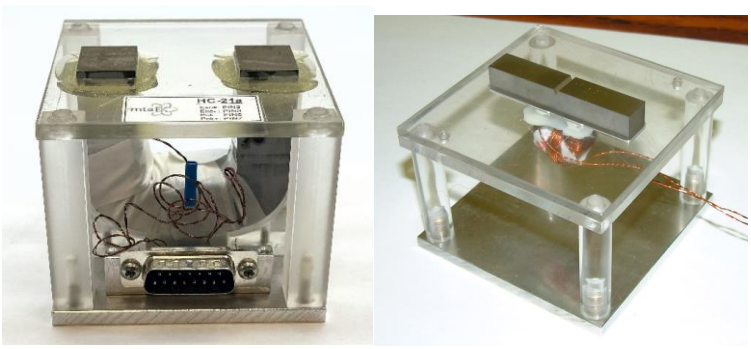

Figure A3. Probes, designed for hot cell MAT measurements. Left: probe for measuring blocks, Right: probe for measuring Charpy samples. (Here a sample is also shown, placed on the top (V-notch is opposite to the magnetizing yoke.).

2. 3MA-X8

Micromagnetic techniques are widely used for the nondestructive characterization of material properties of ferromagnetic steels. They are based on the correlation between the magnetic properties

Preprints (www.preprints.org) | NOT PEER-REVIEWED | Posted: 14 December 2023 doi:10.20944/preprints202312.1008.v1

of ferromagnetic materials and their mechanical-technological characteristics, which are dependent on the microstructure. This correlation is related to the microstructure interaction with both the magnetic structure (domain (Bloch) walls) as well as the dislocations [63-65]. Fraunhofer IZFP has developed the 3MA technique (Micromagnetic Multiparameter Microstructure and Stress Analysis), which indirectly and non-destructively determines mechanical material properties using a one-sided access probe. 3MA is based on a combination of several magnetic methods and has been described in previous studies in detail [63-65]. The latest implementation of 3MA is the 3MA-X8 principle, which has been applied in this work. 3MA-X8 records parameters derived from three micromagnetic methods that rely on a single sensor coil wound on a U-shaped core. The 3MA-X8 probe contains an electromagnet that excites a magnetic field of two superimposed frequencies in the sample. The time domain signals of drive voltage and drive current depend on the sample property contacted by the probe. These signals are analyzed in order to extract up to 21 characteristic features that describe the magnetization behavior and then can be correlated to the mechanical material properties.

The following three micromagnetic methods are used in 3MA-X8: eddy current impedance analyis, incremental permeability analysis and harmonics analysis. They differ in terms of the interaction depth and mechanisms and deliver features that qualitatively correlate with material properties. Figure 5m shows the 3MA-X8 device including the used probes and a PC. The 3MA-X8 device is controlled by the Modular Measuring System (MMS) software. For Charpy samples a standard probe was used and for measuring the block shaped samples a large adapted probe was designed and built up. Sample/probe holders were used to improve reproducibility by minimizing positioning variations.

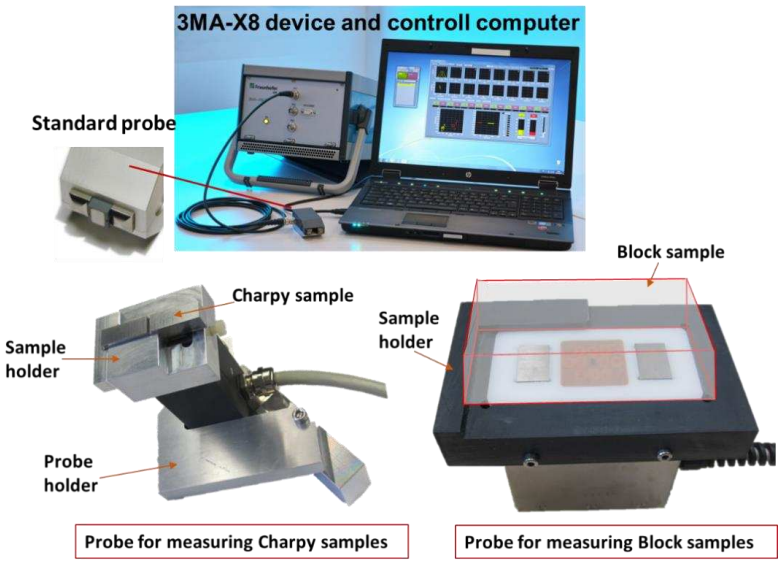

Figure A4. The micromagnetic multiparameter microstructure and stress analysis (3MA)-X8 system, including 3MA-X8 device, standard probe, and PC (top); probe and sample holder for Charpy's (bottom left) and probe and sample holder for block samples (bottom right).

3. MIRBE

The Micromagnetic Inductive Response & Barkhausen Emission (MIRBE) technique is a non-destructive examination technique for microstructural changes, detection of surface defects and case hardening levels [50 60]. In more depth, the method works where magnetic changes over time along with the Bakhausen Noise analysis provides an insight in to the material charcteristcis/properties. MIRBE has its origins from the B-H Hysteresis loop which is not a smooth curve as the magnetic flux density versus the intensity of the magnetic field resultants in a curve that is instead described as a non-linear step function. These steps correlate with the irregular fluctuations in the magnetization when energized from cyclic excitation provided by ferrous yokes to excite the material area under test. These steps or jumps of domains form Barkhausen Noise (BN) and are provided from magnetic

Preprints (www.preprints.org) | NOT PEER-REVIEWED | Posted: 14 December 2023 doi:10.20944/preprints202312.1008.v1

domain motion which is the basis of the Barkhausen signal. Moreover, until the applied field is increased sufficiently, pining sites tend to restrict the moving domain wall. When the applied field is reached, sudden changes in magnetisation result which are produced by the sudden and discontinuous movement of domain walls. In the case of microstructural characteristics "defects" such as dislocations, precipitations and segregations which cause pinning of the moving domain walls and promote Barkhausen signal changes. Barkhausen Noise is measured from a recieiving 'pick-up coil (independent to the energizing yoke)' in the form of a voltage signal significant of surface eddy currents experienced near the surface of the material.

BN measurements were undertaken using a magnetic Barkhausen noise analys-er (Rollscan 350) with a general-purpose sensor developed by Stresstech [115]. The magneto elastic parameter (mp) signifying the RMS (Root Mean Square) value is expressed as a function of the magnetizing voltage, current and frequency. Each measurement consisted of periodic bursts of BN signals for a set duration of ten seconds, and the BN RMS is calculated from such signal bursts. The RMS of the MBN signals is given as:

$$\mathrm{RMS} = \sqrt{\frac{\sum_{i=1}^{n} y_i^{\,2}}{n}}$$

where n is the total number of BN signals captured in the particular frequency range, and yi is the amplitude of the individual burst.

The main instrumentation input parameters are voltage and frequency and these are determined from voltage and frequency sweeps giving an optimum 'trade-off' value for a specific material under test. Both sinusoidal and triangular waveforms can be used to energise the surface, due to saturation issues with the triangular waveform, the sinusoidal waveform was used. It should also be noted, the frequency of the applied field affects the depth at which the Barkhausen Noise reading is obtained. The frequency is inversely proportial to depth of penetration. A penetration depth between 0.01 mm and 1 mm was achieved where a band pass filter of between 70 kHz and 200 kHz was selected for channeling the pick-up signals of interest.

Scatter of magnetic output responses vs. DBTT was also found with Barkhausen noise. It was considered such scatter is due to the material microstructure differences as well surface quality in terms of surface roughness. Measurement uncertainty however was minimized as much as possible, this is in terms of sensor pick-off, surface quality and applied force. The measurement testing regime used a three times sensor pick-off (physical movement of the sensor to and from the same position maintained) followed by 5 measurements each time the sensor touched the sur-face of the material. The MIRBE setup, used for the measurements can be seen in Figure A5.

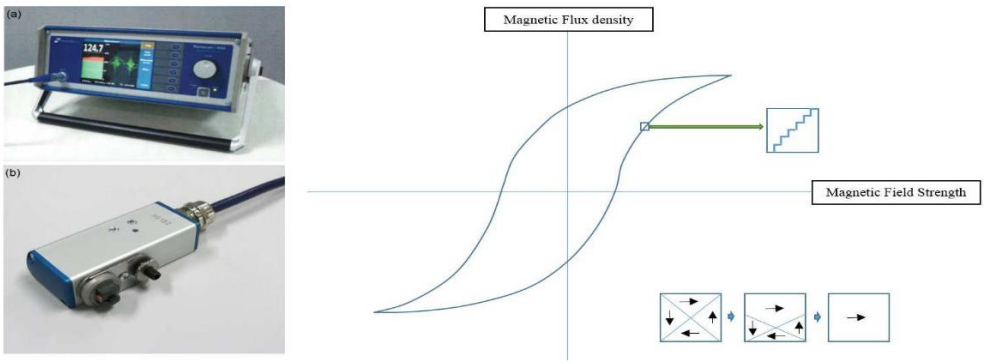

Figure A5. MIRBE setup used in the work (a) noise analyser and (b) sensor (c) Schematic of domain growth during magnetic hysteresis cycle using MIRBE (BN) method.

Appendix B: Interpretation of the scatter of points

The results of different nondestructive measurements are presented in Section 8. As a general conclusion, a reasonable correlation was found between the nondestructively measured magnetic

Preprints (www.preprints.org) | NOT PEER-REVIEWED | Posted: 14 December 2023 doi:10.20944/preprints202312.1008.v1

parameters and the destructively measured transition temperature, regardless on the type of measurement (MAT, 3MA, MIRBE). However, the measurement points significantly scatter in all of these experiments. It has been supposed that the reason of this scatter can be the local material inhomogeneity [114]. It is also known that the embrittlement also depends on the initial material conditions, in spite of the fact that the investigated samples were cut from the same block. Considering the importance of these nondestructive measurements on RPV steel for the potential future inspection of nuclear reactors, the results should be analyzed and verified carefully. This was the purpose of the work, described in Ref. [116], and in this Section the most important results and conclusions are summarized. The results of the measurements presented in Section 8 are also considered here, but these results are evaluated from a different point of view. In Ref. [116] the measurement results of two series of Charpy specimens (made of two different types RPV steel) were analyzed. Measurements were performed before and after neutron irradiation, and the above mentioned three magnetic methods were applied on the same specimens. In this Section only the measurements, made on 15kH2NMFA material are presented, but very similar results were obtained also on A508 Cl.2 material.

The same procedure was taken for a series of blocks, this result is also presented below.

1. Results of MAT, 3MA and MIRBE measurements made on all Charpy samples

1.1. Evaluation of data without normalization

It is shown in Figure B1, how the optimally chosen MAT descriptor depends on DBTT. Similar result of 3MA measurement is shown in Figure B2, while the result of MIRBE measurements can be seen in Figure B3. These results are identical with the results presented in Section 8.

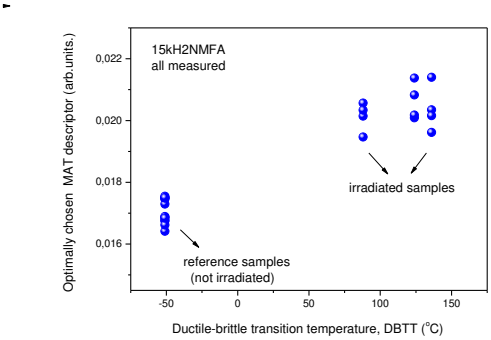

Figure B1. MAT parameter as a function of DBTT for all measured 15kH2NMFA samples.

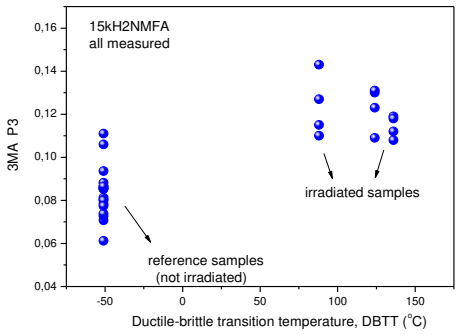

Figure B2. 3MA parameter as a function of DBTT for all measured 15kH2NMFA samples.

Preprints (www.preprints.org) | NOT PEER-REVIEWED | Posted: 14 December 2023 doi:10.20944/preprints202312.1008.v1

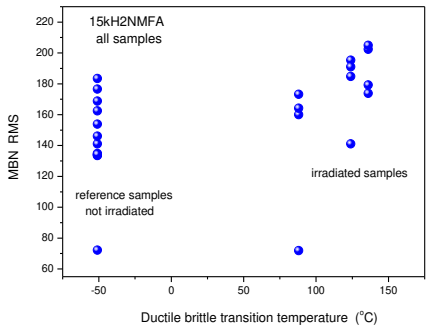

Figure B3. MIRBE parameter as a function of DBTT for all measured 15kH2NMFA samples.

It is evident that neutron irradiation caused well measurable modification of magnetic parameters. A more or less linear correlation seems to exist between magnetic quantities and DBTT. However, the most visible effect is the big scatter of points, regardless on the actual way of measurement.

On the other side, it is also evident in the above figures that even the magnetic parameters of reference (not irradiated) samples scatter a lot. This experience gives a possible explanation of the scatter of points: the samples themselves behave differently, in spite of the fact that they were cut from the same block. Magnetic measurements only reflect this material inhomogeneity. Consequently, it is not surprising that the points scatter also after irradiation. To get an impression about behaviour of *individual* samples, it will be investigated in next subsection, how the magnetic behaviour of individual samples are modified due to neutron irradiation.

1.2. Evaluation of normalized data

In Figs. B1 to B3 the measurement results are given without marking the individual samples. Perhaps a more useful way of presentation is to consider the modification of magnetic parameters for each individual sample. Because of this other graphs are shown in Figs. B4 to B6). In these figures the change of magnetic parameters are given with respect to the same magnetic parameter measured on the same sample before irradiation. It is the reason that the first point (Ratio = 1) is the same for all samples, and the other points are connected with individual samples. These points show how the magnetic parameters of a given sample are modified due to irradiation.

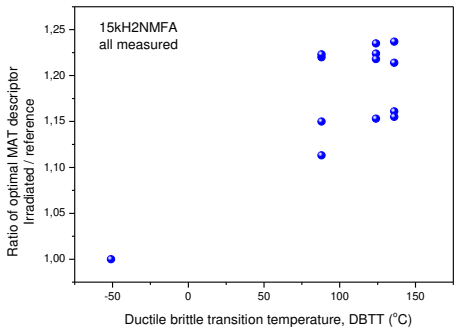

Figure B4. Normalized MAT parameters as function of DBTT for all 15kH2NMFA samples.

Preprints (www.preprints.org) | NOT PEER-REVIEWED | Posted: 14 December 2023 doi:10.20944/preprints202312.1008.v1

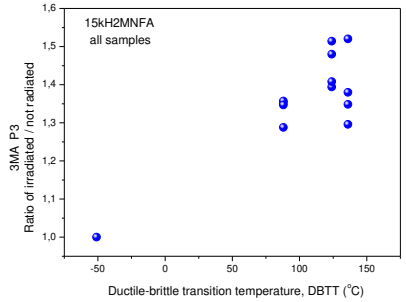

Figure B5. Normalized 3MA parameters as function of DBTT for all 15kH2NMFA samples.

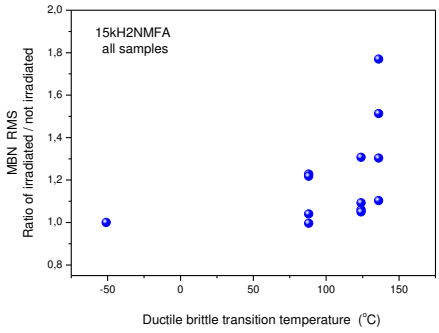

Figure B6. Normalized MIRBE parameters as function of DBTT for all 15kH2NMFA samples.

It is seen very well in the above figures, that the scatter of points is also rather large in the normalized cases. This can be considered as a direct proof that the scatter of points is the result of the originally different behaviour. The neutron irradiation generates different material embrittlement, depending on the individual properties of the samples.

2. Selection of samples

The influence of neutron irradiation is investigated in the above subsections for the case if all measured samples are taken into account. But it is seen very well that even the reference samples are very different from the point of view of magnetic properties. It is not surprising that they also behave differently after irradiation. In this subsection it is shown, how a magnetic selection of samples can be done. This selection is based on permeability measurements of samples. In the next subsection it will be shown, how the correlation between magnetic parameters and DBTT looks like if only the selected samples are taken into account. It is important to emphasize that this selection was made *before* any further magnetic measurement and evaluation of irradiated samples.

The permeability loops were measured on reference samples, before irradiation. This means, that the selection does not take into account the material embrittlement, generated by the neutron irradiation. It reflects simply the behaviour of samples in initial conditions.

No backward reasoning has been used to decide which measured points fit best to our hypothesis. To clarify this statement the details of this selection process are briefly given:

- A large scatter of all magnetic parameters measured on both the reference and irradiated samples we observed.
- Regardless of the result of magnetic measurements, we compared the magnetic behaviour of reference samples were compared to each other. It was found that four samples behaved similarly from the magnetic point of view.
- The MAT, 3MA and MBN evaluations (not measurements!) were repeated, taking into account only those selected samples. It is evident that this selection cannot give any information about the behaviour of the irradiated samples; considering that it is done prior to the irradiation.

Preprints (www.preprints.org) | NOT PEER-REVIEWED | Posted: 14 December 2023 doi:10.20944/preprints202312.1008.v1

The series of permeability loops with increasing magnetization detected on 15kH2NMFA samples can be seen in the left side of Figure B7. In the right side of the figure the magnified parts of the loops are shown. For the sake of better visibility here the envelope of the large amplitude minor loops are shown. The difference between loops are seen well, and an easy selection can be made. Four samples behave similarly: Nos. 172, 173, 178, 183.

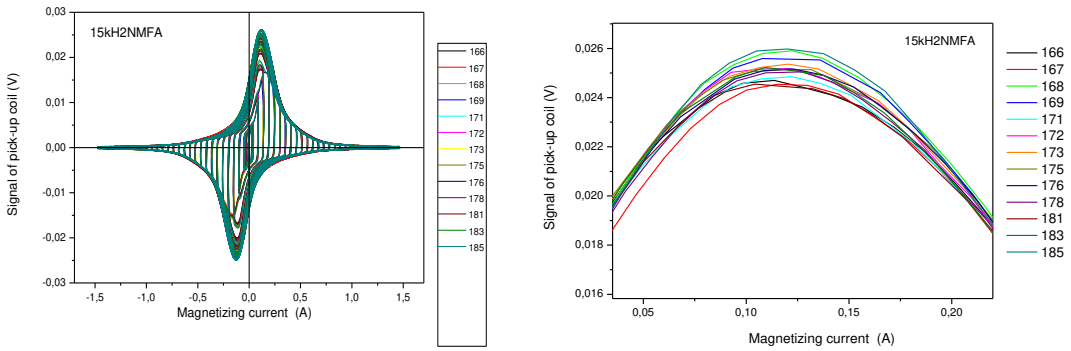

Figure B7. Total permeability loops of 15kH2NMFA samples before irradiation (left). The magnified part of the left graph (right).

3. Results of 3MA, MAT and MBN measurements considering selected samples only

In this subsection it is shown, how the scatter of points looks like if the evaluation of magnetic parameters has been performed by taking into account only the magnetically pre-selected samples. Results can be seen in Figs. B8, B9 and B10, respectively.

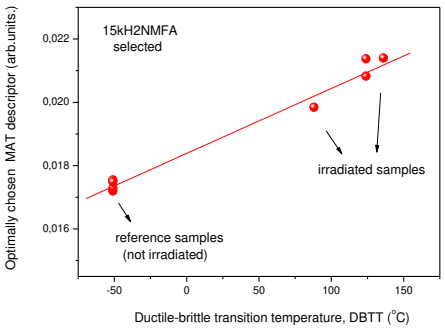

Figure B8. Optimally chosen MAT descriptor as a function of DBTT for selected 15kH2NMFA samples.

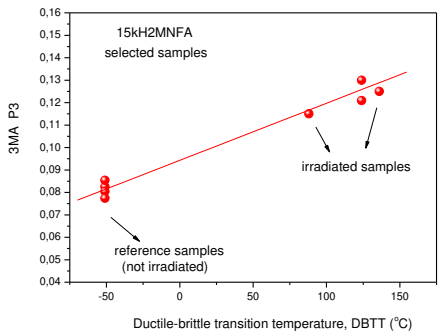

Figure B9. 3MA parameter as a function of transition temperature for selected 15kH2NMFA samples.

Preprints (www.preprints.org) | NOT PEER-REVIEWED | Posted: 14 December 2023 doi:10.20944/preprints202312.1008.v1

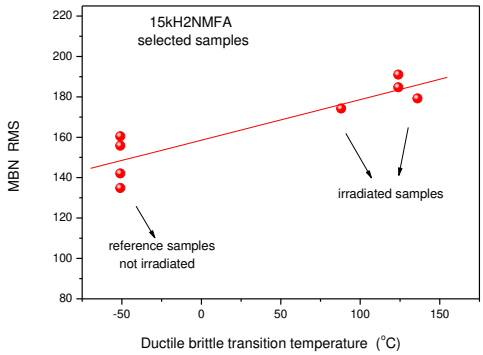

Figure B10. MIRBE parameter as a function of transition temperature for selected 15kH2NMFA samples.

4. Results of MAT measurements made on blocks

In this subsection the results of the same procedure as described above is given, but now those measurements are considered, which were performed on A508 Cl.2 base metal blocks, before and after neutron irradiation [104]. Again, the measurement points are the same as presented in Section 8 but after performing the magnetic selection, and only MAT results are considered. The correlation between MAT parameters and DBTT are shown in Figure B11, before and after selection.

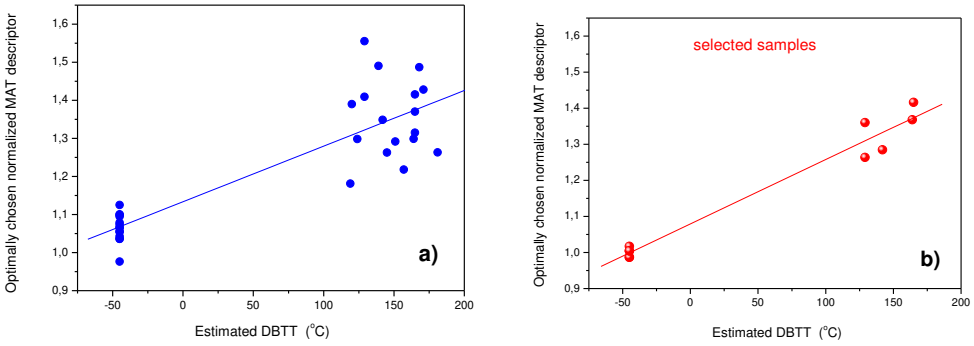

Figure B11. Optimally chosen MAT descriptor as a function of estimated DBTT on all base material samples (a), and the same correlation after magnetic selection (b).

5. Discussion

The above described analysis revealed that the experienced big scatter is most probable connected with the different behaviour of samples. The measurement errors of the applied magnetic methods are not responsible for this scatter. In case of MAT a careful analysis of potential experimental errors was performed [114] and it was found that by taking into account of all possible sources of uncertainty, the error of the whole MAT evaluation is less than 1%.

By comparing Figs. B8-B10 with either Figs. B1-B3 or with Figs. B4-B6 it is clearly seen that the scatter of points significantly decreased if the evaluation of measurement results was performed only on the selected Charpy samples. Obviously, a linear correlation with low scatter of points was found between magnetic parameters and DBTT. This statement is supported by the fact that all the three applied methods resulted the same: Neither the correlation between magnetic quantities and transition temperature, nor the scatter do not depend on the actual way of measurement. This fact is very promising for the future practical application of magnetic methods. Results of different methods verify each other.

 doi:10.20944/preprints202312.1008.v1

Furthermore, the influence of proper magnetic selection is identical for both Charpy and block samples. This fact makes evident that this phenomenon also does not depend on the size and shape of investigated specimens.

6. Conclusions

It was clearly demonstrated by our experiments, that the neutron irradiation-generated embrittlement is very well characterized with low scatter of measured magnetic parameters if the parameters of the not irradiated samples are close to each other. The selection can be easily performed by magnetic measurements.

It can be stated – based on the above experimental results - that magnetic parameters seem to characterize better the neutron irradiaton induced material embrittlement than the traditionally used destructive methods, e.g. transition temperature. This is the most important conclusion of this work. The scatter of the magnetic parameters is significantly lower than the scatter of destructive Charpy impacts tests. Furthermore, the magnetic measurements characterize the individual samples, in contrary to the DBTT values determined by the Charpy method, which provides only statistical values on the sample sets.

Another important conclusion was also found that the local material inhomogeneity influence a lot the neutron irradiation-generated material embrittlement. Different parts of RPV, even if they are cut from the same block, are hardened differently. Local material conditions are responsible for the different embrittlement of the material caused by the same dosage of neutron irradiation.

These results mean a serious argument for the application of magnetic measurements in the reactor industry in the future.

References

1. The Economics of Long-term Operation of Nuclear Power Plants, Nuclear Development 2012, NUCLEAR ENERGY AGENCY and ORGANISATION FOR ECONOMIC CO-OPERATION AND DEVELOPMENT, ISBN 978-92-64-99205-4.
2. Keim E., Lidbury D.: Review of assessment methods used in nuclear plant lifetime management, report based on contributions by members of NULIFE Expert Groups 2 and 3, Report No. Nullife 12 (5), May 2012.
3. Ballesteros, A.; Ahlstrand, R.; Bruynooghe, C.; von Estorff, U.; Debarberis, L.. *Nucl. Eng. Des,*. **2012**, *243*, 63–68.
4. Al Mazouzi, A.; Alamo, A.; Lidbury, D.; Moinereau, D.; Van Dyck, S., *Nucl. Eng. Des*., **2011**, *241*, 3403–3415.
5. Koutsky, J.; Kocık, J. Radiation Damage of Structural Materials; Elsevier: Amsterdam, The Netherlands, **1994.**
6. Ferreño, D.; Gorrochategui, I.; Gutiérrez-Solana, F. Degradation due to neutron embrittlement of nuclear vessel steels: A critical review about the current experimental and analytical techniques to characterise the material, with particular emphasis on alternative methodologies. In *Nuclear Power—Control, Reliability and Human Factors*;
7. https://inis.iaea.org/collection/NCLCollectionStore/_Public/07/222/7222068.pdf
8. https://www.astm.org/stp909-eb.html
9. Steele L.E., Potapovs U., *Nuclear Engineering and Design*, **1968**, *8*, 58
10. Odette G.R., Lucas G.E., Recent progress in understanding reactor pressure vessel steel embrittlemen,t Rad. Effects and Defects in Solids, 1998, 144, 189.
11. Odette G.R., Lucas G.E., JOM, 2001, 53, 18.
12. Odette GR, Nanstad RK. Predictive reactor pressure vessel steel irradiation embrittlement model: issues and opportunities. J Metals. 2009;61:17–23
13. Debarberis L., Kryukov A., Gillemot F., Valo M., Morozov A., Brumovsky M., Acosta B., Sevini F., Strength of Materials, 2004, 36, 269.
14. Phythian WJ, English CA. Microstructural evolution in reactor pressure vessel steels. J Nucl Mater. 1993;205:162–177.
15. Scott P. A review of irradiation assisted stress corrosion cracking. J Nucl Mater. 1994;211:101–122.
16. Bruemmer SM, Simonen EP, Scott PM, Andresen PL, Was GS, Nelson JL. Radiation-induced material changes and susceptibility to intergranular failure of light-water-reactor core internals. J Nucl Mater.;274:299–314.
17. Was GS, Andresen PL. Stress corrosion cracking behavior of alloys in aggressive nuclear reactor core environments. Corrosion. 2007;63:19–45.

18. Chopra OK, Rao AS. A review of irradiation effects on LWRcore internalmaterials – IASCC susceptibility and crack growth rates of austenitic stainless steels. J Nucl Mater. 2011;409:235–256.
19. Wallin, K., "The Scatter in KIc results," Engineering Fracture Mechanics, Vol. 19, (1984) 1085-1093.
20. AMERICAN SOCIETY FOR TESTING AND MATERIALS, Test Method for Determination of Reference Temperature, T0, for Ferritic Steels in the Transition Range, ASTM, West Conshohocken, PA, Vol. 03.01, ASTM E 1921 (2002).
21. Server, W.L., et al., "Application of master curve fracture toughness for reactor pressure vessel integrity assessment in the USA", presented at IAEA Specialists Meeting, Gloucester, UK, 2001.
22. Debarberis L., Kryukov A., Gillemot F., Acosta B., Sevini F., International Journal of Pressure Vessels and Piping, 2005, 82, 195.
23. Gillemot F., Horváth Á., Horváth M., et. al., Microstructural changes in highly irradiated 15H2MFA steel, 26th Symposium on the Effects of Radiation on Nuclear Materials. ASTM STP, 2014, Paper ID STP-2013-0098.
24. Kryukov A., Debarberis L., von Estorff U., Gillemot F., Oszvald F., Journal of Nuclear Materials, 2013. 422, 173.
25. Trampus, P. Pressurized Thermal Shock Analysis of the Reactor Pressure Vessel. Procedia Struct. Integr. 2018, 13, 2083–2088.
26. Chen, M.; Yu, W.; Qian, G.; Shi, J.; Cao, Y.; Yu, Y. Crack Initiation, Arrest and Tearing Assessments of a RPV Subjected to PTS Events. Ann. Nucl. Energy 2018, 116, 143–151.
27. Fukuya K., Current understanding of radiation-induced degradation in light water reactor structural materials, Journal of Nuclear Science and Technology, 2013, 50, 213–254.
28. P.K.Liaw, W.G.Clark Jr., R.Rishel, D.Drinon, M.K.Devine and D.C.Jiles , Life prediction and nondestructive evaluation of materials properties in the power plant industry, Proceeding of the First International Conference on microstructures and mechanical properties of aging materials, Chicago, November 1992, p.345. Edited by P.K.Liaw, R.Viswanathan, K.L.Murty, D.Frear and E.P.Simonen
29. Frankfurt, Vladimir; Kupperman, David, Review of electromagnetic NDT methods for monitoring the degradation of nuclear reactor components, 2001 Argonne National Laboratory, Scientific publications
30. Wang X., Qiang W., Shu G., Magnetic non-destructive evaluation of hardening of cold rolled reactor pressure vessel steel, Journal of Nuclear Materials, 2017, 492, 178-182
31. S. Takahashi, S. Kobayashi, H. Kikuchi, Y. Kamada, "Relationship between mechanical and magnetic properties in cold rolled low carbon steel", J. Appl. Phys. (2006) vol.100, p.113908
32. I. Tomáš, J. Kadlecová, R. Konop, M. Dvořáková, "Magnetic nondestructive indication of varied brittleness of 15Ch2MFA steel", Proceedings of 9th International Conference on Barkhausen Noise and Micromagnetic Testing (ICBM9), Hejnice, Czech Republic, June 2011, ISBN 978-952-67247-4-4 (paperback), ISBN 978-952-67247-5-1 (CD-ROM), pp.55-63
33. Seiler, G. Early detection of fatigue at elevated temperature in austenitic steel using electromagnetic ultrasound transducers. In Proceedings of the Seventh International Conference on Low Cycle Fatigue: LCF7, Deutscher Verband für Materialforschung und-prüfung e.V. (DVM), Aachen, Germany, 9–11 September 2013; pp. S359–S364.
34. Smith, R.L.; Rusbridge, K.L.; Reynolds, W.N.; Hudson, B. Ultrasonic attenuation, microstructure and ductile to brittle transition temperature in Fe-C alloys. Mater. Eval. 1993, 41, 219–222.
35. Dobmann, G.; Kröning, M.; Theiner, W.; Willems, H.; Fiedler, U. Nondestructive characterization of materials (ultrasonic and magnetic techniques) for strength and toughness prediction and the detection early creep damage. Nucl. Eng. Des. 1995, 157, 137–158.
36. E. Schneider: Ultrasonic Technique; In: Hauk, V.: Structural and Residual Stress Analysis by Nondestructive Methods: Evaluation - Application – Assessment, In: Amsterdam: Elsevier, S. 522-563, 1997.
37. H. Willems and K. Goebbels, "Characterization of microstructure by backscatter ultrasonic waves", Material Science, Vol.15, 191, pp. 549-553.
38. Niffenegger, M, Mora, DF, & Kottmann, H. "Non-Destructive Evaluation of RPV Embrittlement by Means of the Thermoelectric Power Method." Proceedings of the Volume 7: Non-Destructive Examination. Virtual, Online. August 3, 2020. V007T07A002. ASME. https://doi.org/10.1115/PVP2020-21446
39. Niffenegger, M.; Leber, H.J. Monitoring the embrittlement of reactor pressure vessel steels by using the Seebeck coefficient. J. Nucl. Mater. 2009, 389, 62.
40. Niffenegger, M.; Reichlin, K.; Kalkhof, D. Application of the Seebeck effect for monitoring of neutron embrittlement and low-cycle fatigue in nuclear reactor steel. Nucl. Eng. Des. 2005, 235, 1777–1788.
41. M. Valo, P. Lappalainen, T. Lyytikäinen, J.Lydman, M.Paasila, (2013) Advanced surveillance technique and embrittlement modelling (SURVIVE), In: SAFIR2014. The Finnish Research Programme on Nuclear Power Plant Safety 2011-2014. Interim Report. Simola, Kaisa (ed.). VTT Technology 80, VTT, Espoo, http://www.vtt.fi/inf/pdf/technology/2013/T80.pdf , pp. 313-323.
42. T. Planman, M. Valo, P. Lappalainen, K. Wallin, (2014), Variability of material properties in Greifswald NPP beltline welds (P07), IGRDM 18, Int. Gr. Radiat. Damage Mechanisms, 23 - 28 Nov. 2014, Miyazaki, Japan

43. Kronmüller, H.; Fähnle, M. Micromagnetism and the Microstructure of Ferromagnetic Solids; Cambridge University Press: Cambridge, UK, 2003.
44. Devine, M.K. Magnetic detection of material properties. J. Min. Met. Mater. JOM 1992, 44, 24–30
45. D.C. Jiles, Review of magnetic methods for nondestructive evaluation",. NDT International, 21, 311, 1988
46. Blitz, J. Electrical and Magnetic Methods of Nondestructive Testing; Adam Hilger IOP Publishing, Ltd.: Bristol, UK, 1991.
47.] Jiles, D.C. Magnetic methods in nondestructive testing. In Encyclopedia of Materials Science and Technology; Buschow, K.H.J., Ed.; Elsevier: Oxford, UK, 2001; p. 6021.
48. Johnson M.J, Lo C.C.H.,Zhu B., Cao H., Jiles D.C., Magnetic measurements for NDE: background, implementation and applications, Journal of Nondestructive Evaluation, 20, 11, 2000
49. Kempf R.A, Sacanell J., Milano J., Guerra Méndez N., Winkler E., ButeraA., Troiani H., Saleta M.E., Fortis A.M., Correlation between radiation damage and magnetic properties in reactor vessel steels, Journal of Nuclear Materials, 2014, 445, 57-62
50. Rudyak V.M., The Barkhausen effect, Sov. Phys. Usp. 1971, 13 461
51. Lo, C.C.H.; Jakubovics, J.P.; Scrub, C.B. Non-destructive evaluation of spheroidized steel using magnetoacoustic and Barkhausen emission. IEEE Trans. Magn. 1997, 33, 4035–4037.
52.] Kikuchi, H.; Ara, K.; Kamada, Y.; Kobayashi, S. Effect of microstructure changes on Barkhausen noise properties and hysteresis loop in cold rolled low carbon steel. IEEE Trans. Magn. 2009, 45, 2744–2747
53. Hartmann, K.; Moses, A.J.; Meydan, T. A system for measurement of AC Barkhausen noise in electrical steels. J. Magn. Magn. Mater. 2003, 254–255, 318–320.
54. Kadavath, G.; Mathew, J.; Gri_n, J.; Parfitt, D.; Fitzpatrick, M.E. Magnetic Barkhausen Noise Method for Characterisation of Low Alloy Steel. In Proceedings of the ASME Nondestructive Evaluation, Diagnosis and Prognosis Division (NDPD), San Antonio, TX, USA, 14–19 July 2019; ASME: New York, NY, USA, 2019
55. Liu, T.; Kikuchi, H.; Kamada, Y.; Ara, K.; Kobayashi, S.; Takahashi, S. Comprehensive analysis of Barkhausen noise properties in the cold rolled mild steel. J. Magn. Magn. Mater. 2007, 310, e989–e991.
56.] Ktena, A.; Hristoforou, E.; Gerhardt, G.J.L.; Missell, F.P.; Landgraf, F.J.G.; Rodrigues, D.L.; Alberteris-Campos, M., Barkhausen noise as a microstructure characterization tool, Physica B 2014, 435, 109–112.
57. D.Clatterbuck, M.J.Johnson, D.C.Jiles and V.Garcia, Modeling the magnetic Barkhausen effect, Review of Progress in Quantitative NDE, 19, 1533, 2000
58. Jeong, H.T., Park, D.G., Hong, J.H., Ahn, Y.S., Kim, G.M., The effect of microstructural changes on magnetic Barkhausen noise in Mn-Mo-Ni pressure vessel steel, Journal of the Korean Physical Society; 1999, 34(5), 429-433
59. Park D.G., Ok C.I., Jeong H.T., Kuk I.H., Hong J.H., Nondestructive evaluation of irradiation effects in RPV steel using Barkhausen noise and magnetoacoustic emission signals, Journal of Magnetism and Magnetic Materials, 1999, 196-197, 382-384
60. JW Wilson, N Karimian, W Yin, J Liu, CL Davis, AJ Peyton, Magnetic sensing for microstructural assessment of power station steels: Magnetic Barkhausen noise and minor loop measurements, Journal of Physics: Conference Series 450 (2013) 012041 doi:10.1088/1742-6596/450/1/012041
61. R. Ranjan, D.C. Jiles and P.K. Rastogi, Magnetoacoustic emission, magnetisation and Barkhausen effect in decarburised steel, IEEE Transactions on Magnetics, MAG-22, 511, 1986
62. Augustyniak, B.; Chmielewski, M.; Piotrowski, L.; Kowalewski, Z. Comparison of properties of magnetoacoustic emission and mechanical barkhausen effects for P91 steel after plastic flow and creep. IEEE Trans. Magn. 2008, 44, 3273–3276.
63. Dobmann, G.; Altpeter, I.; Kopp, M.; Rabung, M.; Hubschen, G. ND-materials characterization of neutron induced embrittlement in German nuclear reactor pressure vessel material by micromagnetic NDT techniques. In Electromagnetic Nondestructive Evaluation (XI); IOS Press: Amsterdam, The Netherlands, 2008; p. 54, ISBN 978-1-58603-896-0.
64. Altpeter, I.; Becker, R.; G Dobmann, R.; Kern, W.A.; Theiner, A. Yashan: Robust Solutions of Inverse Problems in Eletromagnetic Non-Destructive Evaluation. Inverse Probl. 2002, 18, 1907–1921.
65. Szielasko, K.; Wolter, B.; Tschuncky, R.; Youssef, S. Micromagnetic materials characterization using m7schin learning—Progress in Nondestructive Prediction of Mechanical Properties of Steel and Iron. Tech. Mess. 2020, 87, 428–437.
66. D.C. Jiles and J.B. Thoelke, Theory of ferromagnetic hysteresis: determination of model parameters from experimental hysteresis loops, IEEE Trans. Mag. 25, 3928, 1989.
67. Vandenbossche, L., 2009. Magnetic Hysteretic Characterization of FerromagneticMaterials with Objectives Towards Non-Destructive Evaluation of MaterialDegradation. Gent University, Gent, Belgium (PhD Thesis).
68. Satoru Kobayashi; Nobuhiro Kikuchi; Seiki Takahashi; Yasuhiro Kamada; Hiroaki Kikuchi, Magnetic properties of α'martensite in austenitic stainless steel studied by a minor-loop scaling law, Journal of Applied Physics 108, 043904 (2010)

69. Tomáš I., Non-destructive Magnetic Adaptive Testing of ferromagnetic materials. J. Magn. Magn. Mat. 2004, 268, 178–185
70. Tomáš, I.; Vértesy, G. Magnetic adaptive testing. In Nondestructive Testing Methods and New Applications; Omar, M., Ed.; IntechOpen Limited: London, UK, 2012; ISBN 978-953-51-0108-6. Available online: http://www.intechopen.com/articles/show/title/magnetic-adaptive-testing
71. Vértesy, G., Tomás, I., Takahashi, S., Kobayashi, S., Kamada, Y., Kikuchi, H., Inspection of steel degradation by Magnetic Adaptive Testing, NDT&E Int., 2008. 41, 252–257
72. G. Vértesy, I. Mészáros, I. Tomáš, Nondestructive magnetic characterization of TRIP steels, NDT & E INTERNATIONAL, 54 (2013) 107–114
73. Gillemot F., Pirfo Barroso S. (2010) Possibilities and difficulties of the NDE evaluation of irradiation degradation, Proceedings of 8th International Conference on Barkhausen Noise and Micromagnetic Testing (ICBM8) (ISBN 978-952-67247-2-0)
74. B. Minov, „Investigation of the hardening in neutron irradiated and thermally aged iron-copper alloys, on the basis of mechanical and magnetic relaxation phenomena“, Gent University, Gent, Belgium, PhD Thesis 2012
75. Vandenbossche, L., Konstantinović, M.J., Dupré, L., Magnetic hysteretic characterization of the irradiation-induced embrittlement of Fe, Fe–Cu model alloys, and reactor pressure vessel steel, J. Mag. Mag. Mater. 2008, 320, 562–566
76. Li C., Shu G., Xu B., Liu Y., Chen J., Liu W., Effects of neutron irradiation on magnetic properties of reactor pressure vessel steel, Nuclear Engineering and Design, 2019, 342, 128-132
77. Park D.G., Moon E.J., Kim D.J., Chi S.H., Hong J.H., The change of saturation magnetization in neutron-irradiated low-alloy steel, Physica B, 2003, 327 , 315-318
78. Chi S.H., Chang K.O., Hong J.H., Kuk I.H., Changes in magnetic parameters of neutron irradiated SA 508 Cl. 3 reactor pressure vessel forging and weld surveillance specimens, J. Appl. Phys., 1999, 85, 5726-5728
79. L.B. Sipahi, M.R. Govindarju, D.C. Jiles, Monitoring neutron embrittlement in nuclear pressure vessel steels using micromagnetic Barkhausen emissions, J. Appl. Phys., 1994, 85, 6981-6983
80. Y.Y. Song, D.G. Park, J.H. Hong, The effect of microstructural changes on magnetic Barkhausen noise and magnetomechanical acoustic emission in Mn–Mo–Ni pressure vessel steel, J. Appl. Phys., 87 (2000), pp. 5242-5245
81. Duck-Gun Park; Hee-Tae Jeong; Jun-Hwa Hong, A study on the radiation damage and recovery of neutron irradiated vessel steel using magnetic Barkhausen noise, *Journal of Applied Physics* 85, 5726–5728 (1999)
82. Barroso, S.P.; Horváth, M.; Horváth, Á. Magnetic measurements for evaluation of radiation damage on nuclear reactor materials. Nucl. Eng. Des. 2010, 240, 722–725
83. F. Gillemot, S. Pirfo Barroso, "Possibilities and difficulties of the NDE evaluation of irradiation degradation", Proceedings of 8th International Conference on Barkhausen Noise and Micromagnetic Testing (ICBM8), 2010, (ISBN 978-952-67247-2-0)
84. J.S. McCloy; Pradeep Ramuhalli; Charles Henager, Jr. Use of first order reversal curve measurements to understand Barkhausen noise emission in nuclear steel, *AIP Conference Proceedings* 1511, 1709–1716 (2013), https://doi.org/10.1063/1.4789247
85. Kobayashi S., Kikuchi H., Takahashi S., Kamada Y., Ara K., Yamamoto T., Klingensmith D., Odette, G.R., The effect of copper and manganese on magnetic minor hysteresis loops in neutron irradiated Fe model alloys, Journal of Nuclear Materials, 2009, 384, 109-114
86. S. Takahashi, H. Kikuchi, K. Ara, N. Ebine, Y. Kamada, S. Kobayashi, M. Suzuki, "In situ magnetic measurements under neutron radiation in Fe metal and low carbon steel", J. Appl. Phys. (2006) Vol. 100, p.023902
87. S. Kobayashi, H. Kikuchi, S. Takahashi, Y. Kamada, K. Ara, T. Yamamoto, D. Klingensmith, G.R. Odette, Neutron irradiation effects on magnetic minor hysteresis loops in nuclear reactor pressure vessel steels, Philosophical Magazine, 2008, 88, 1791–1800
88. S. Kobayashi, T. Yamamoto, D. Klingensmith, G.R. Odette, H. Kikuchi, Y. Kamada, Magnetic evaluation of irradiation hardening in A533B reactor pressure vessel steels: Magnetic hysteresis measurements and the model analysis, Journal of Nuclear Materials, 2012, 422, 158-162
89. S. Kobayashi, F. Gillemot, Á. Horváth, R. Székely, „Magnetic properties of a highly neutron-irradiated nuclear reactor pressure vessel steel“, Journal of Nuclear Materials 421 (2012) 112-116
90. Tomáš, I., Vértesy, G., Gillemot, F., Székely, R., Nondestructive Magnetic Adaptive Testing of nuclear reactor pressure vessel steel degradation. J. Nucl. Mater. 2013, 432, 371–377
91. Tomáš I., Vértesy G., Pirfo Barroso S., Kobayashi S., Comparison of four NDT methods for indication of reactor steel degradation by high fluences of neutron irradiation, Nuclear Engineering and Design, 2013, 265 201-209
92. I. Tomáš, J. Kadlecová, G. Vértesy, Measurement of flat samples with rough surfaces by Magnetic Adaptive Testing, IEEE Trans Magn, 48 (2012) 1441-1444

93. G. Dobmann, I. Altpeter, M. Kopp, M. Rabung, G. Hubschen, "ND-materials characterization of neutron induced embrittlement in German nuclear reactor pressure vessel material by micromagnetic NDT techniques", Electromagnetic Nondestructive Evaluation (XI), 2008, p.54, IOS Press, ISBN 978-1-58603-896-0
94. G. Dobmann, "Non-Destructive Testing for Ageing Management of Nuclear Power Components", in Nuclear Power - Control, Reliability and Human Factors, P.Tsvetkov (Ed.), ISBN: 978-953-307-599-0, InTech (2011), Available from: http://www.intechopen.com/articles/show/title/non-destructive-testing-for-ageing-management-of-nuclear-power-component
95. http://www.nomad-horizon2020.eu
96. Uytdenhouwen, R. Chaouadi and other NOMAD consortium members, "NOMAD: Non-destructive Evaluation (NDE) system for the inspection of operation-induced material degradation in nuclear power plants – overview of the neutron irradiation campaigns", Proc. Of the ASME 2020, Vol. 7: Non-destructive examination, V007T07A003, PVP2020-21512
97. Uytdenhouwen, R. Chaouadi, "Effect of neutron irradiation on the mechanical properties of an A508 Cl.2 forging irradiated in a BAMI capsule", Proc. ASME 2020, Vol. 1: Codes and standards, V001T01A060, PVP2020-21513.
98. Uytdenhouwen, R. Chaouadi, To be published in the ASME 2021 proceedings PVP2021-61969 paper: Effect of neutron irradiation on the mechanical properties of an A508 Cl.2 and 15Kh2NMFA irradiated in the NOMAD_3 rig in the BR2 cooling water
99. Nondestructive Evaluation (NDE) System for the Inspection of Operation-Induced Material Degradation in Nuclear Power Plants, (GA 755330) DOI 10.3030/755330, Parametric study, Documents download module (europa.eu)
100. Rabung, M.; Kopp, M.; Gasparics, A.; Vértesy, G.; Szenthe, I.; Uytdenhouwen, I.; Szielasko, K. Micromagnetic Characterization of Operation-Induced Damage in Charpy Specimens of RPV Steels. Appl. Sci. 2021, 11, 2917.
101. Vértesy G., Gasparics A., Szenthe I., Gillemot F., Uytdenhouwen I., Inspection of Reactor Steel Degradation by Magnetic Adaptive Testing, Materials 2019, 12, 963
102. Vértesy G., Gasparics A., Szenthe I., Bilicz S., Magnetic Investigation of Cladded Nuclear Reactor Blocks, Materials, 2022, 15, 1425
103. G. Vértesy, A. Gasparics, I. Szenthe, F. Gillemot, Magnetic nondestructive inspection of reactor steel cladded blocks, GLOBAL JOURNAL OF ADVANCED ENGINEERING TECHNOLOGIES AND SCIENCES, 6(6): June, 2019, pp. 1-9, ISSN 2349-0292, DOI: 10.5281/zenodo.3246763, http://www.gjaets.com/Issues%20PDF/Archive-2019/June-2019/1.pdf
104. Vértesy G., Gasparics A., Szenthe I., Uytdenhouwen I., Investigation of the Influence of Neutron Irradiation on Cladded Nuclear Reactor Pressure Vessel Steel Blocks by Magnetic Adaptive Testing, Appl. Sci. 2022, 12, 2074
105. Sonja Grönroos "Machine learning in nondestructive estimation of neutron-induced reactor pressure vessel embrittlement" Master's thesis Materials research, Computational materials physics, November 26, 2020 - https://helda.helsinki.fi/handle/10138/328799
106. S. M. Ross, Introductory Statistics, in: S. M. Ross (Ed.), Introductory Statistics (Fourth Edition), fourth edition Edition, Academic Press, Oxford, 2017, pp. 797{800. doi:https://doi.org/10.1016/B978-0-12-804317-2.00031-X
107. R. Kohavi, A Study of Cross-Validation and Bootstrap for Accuracy Estimation and Model Selection, Proceedings of the 14th International Joint Conference on Artificial Intelligence - Volume 2 (1995) 1137-1143. Morgan Kaufmann Publishers Inc.
108. Combination of Non-Destructive Methods in Estimating Irradiation-Induced Reactor Pressure Vessel Steel Alloy Embrittlement with Machine Learning by Sonja Grönroos, Jari Rinta-aho, Tuomas Koskinen, Gonçalo Sorger – SSRN - https://papers.ssrn.com/sol3/papers.cfm?abstract_id=3993039
109. James. M. Griffin, Jino. Mathew, Antal Gasparics, Gábor Vértesy, Inge Uytdenhouwen, Rachid. Chaouadi and Michael E. Fitzpatrick, "Machine-Learning Approach to Determine Surface Quality on a Reactor Pressure Vessel (RPV) Steel", in: MDPI Applied Sciences 2022, 12, 3721. https://doi.org/10.3390/app12083721 https://www.mdpi.com/journal/applsci
110. P. J. Huber, Robust Estimation of a Location Parameter, The Annals of Mathematical Statistics 35 (1) (1964) 73 { 101. doi:10.1214/aoms/1177703732
111. A. J. Smola, B. Sch◉olkopf, A tutorial on support vector regression, Statistics and computing 14 (3) (2004) 199-222
112. K. P. Murphy, Machine Learning: A Probabilistic Perspective, The MIT Press, 2012.
113. Preisach F. Uber die magnetische Nachwirkung, Zeit. fur Physik 1935, Vol. 94 p. 277
114. Gábor Vértesy, Antal Gasparics, Ildikó Szenthe, Inge Uytdenhouwen, Interpretation of Nondestructive Magnetic Measurements on Irradiated Reactor Steel Material, *Appl. Sci.* 2021, *11*, 3650

115. Stresstech Group. Microscan software, Operating Instructions, V.4.4.0. 2016. Available online: (accessed on 15 Fabruary 2019).
116. Vértesy, G.; Gasparics, A.; Szenthe, I.; Rabung, M.; Kopp, M.; Griffin, J.M., Analysis of Magnetic Nondestructive Measurement Methods for Determination of the Degradation of Reactor Pressure Vessel Steel. Materials, **2021**, 14, 5256
117.